Title: Separating good from bad – a methodological assessment of the critical temperature that separates stressful and permissive temperatures in ectotherms.

Authors: Andreas Havbro Faber[1], Frederik Due Møller[2], Bodil Kirstine Ehlers[1], Michael Ørsted[3], Johannes Overgaard[2].

Andreas H Faber[1,*] (AHF, faberhavbro@outlook.dk, ORCiD: 0000-0003-3356-7591)

Frederik Due Møller[2] (FDM, 202109745@post.au.dk)

Bodil Kirstine Ehlers[1] (BE, boe@ecos.au.dk, ORCiD: 0000-0002-4712-5025)

Michael Ørsted[3] (MØ, moer@bio.aau.dk, ORCiD: 0000-0001-8222-8399)

Johannes Overgaard[2] (JO, johannes.overgaard@bio.au.dk, ORCiD: 0000-0002-2851-4551)

Affiliations

[1]Section for Terrestrial Ecology, Department of Ecoscience, Aarhus University, Aarhus C, Denmark.

[2]Section for Zoophysiology, Department of Biology, Aarhus University, Aarhus C, Denmark.

[3]Section of Functional Ecology and Genomics, Department of Chemistry and Bioscience, Aalborg University, Aalborg E, Denmark

[*]Contact author to whom correspondence should be addressed: faberhavbro@outlook.dk, Address: C.F. Møllers Allé 4, 8000 Aarhus C, Denmark. Phone: +4522198915

Acknowledgements

We thank Quintin Geissmann and Markus Dahl Lauritsen giving advice for growing and maintaining the *L. gibba* culture and solving general logistical challenges during the work.

Author contributions

AHF, BKE, FDM, JO and MØ planned and designed the research. AHF performed experiments related to *Lemna gibba*. FDM and JO performed experiments related to *Drosophila suzukii*. AHF, FDM and JO analysed the data. AHF drafted the first version of the manuscript with guidance from JO, and all authors contributed to and revised the manuscript.

Data availability

The data used in this manuscript will be made available on https://figshare.com upon acceptance of the manuscript for publication. Before publishing, reviewers can use this link for assessing the data: https://figshare.com/s/fa878b75e03af2d624e3

Funding

This work was supported by the Independent Research Fund Denmark (grants DFF-1026-00173B to BKE, DFF-4251-00089B to MØ, and DFF-9040-00348B to JO) and the Novo Nordisk Foundation (grant NNF23OC0082599 to MØ).

Abstract

- **Context and aim**: Estimating the thermal limits of ectothermic organisms is critical for predicting their responses to climate change. A key physiological threshold in this context is the critical temperature (T_c), which separates the permissive temperature range, where organisms maintain homeostasis and complete their life cycle, from the stressful range, where thermal stress causes physiological disruption and eventually mortality. We aimed to evaluate experimental methods for estimating T_c in ectotherms and assess their practical utility.
- **Methods**: We evaluated four experimental methods to estimate T_c under heat stress in two model ectotherms, the aquatic plant *Lemna gibba* and the insect *Drosophila suzukii*. Two methods identify T_c as the end-points of either the classic thermal performance curve, or the thermal death time curve, whereas the other two exploit the antagonistic injury-repair processes above and below T_c.
- **Results**: For both species, three of the four methods that vary in exposure duration and temperature intensity all successfully produced consistent T_c estimates, while one failed to identify T_c. When comparing practical aspects of different methodologies, we find that an assay combining high constant temperature assays interrupted by lower temperatures offer a fast and practical method for estimating T_c. Collectively, T_c coincided with the temperature at which performance declined sharply and mortality increased, supporting its interpretation as a biologically meaningful upper thermal limit for ectotherms.
- **Conclusions**: T_c represents a standardized physiological threshold reflecting the physiological transition from sustained homeostasis to the accumulation of acute thermal damage. Its consistent estimation across methods highlights its utility for comparing thermal limits across studies and species. We propose that T_c should be adopted as a standardized

parameter for quantifying upper thermal limits and assessing organismal vulnerability in a warming world.

Keywords: critical temperature, *Drosophila suzukii*, *Lemna gibba*, permissive temperature, stressful temperature, thermal death time curve, thermal tolerance

Introduction

Temperature strongly influences the lifespan and biological processes of ectothermic organisms, shaping not only how they perform in their environment but also their rate of mortality if temperatures exceed their thermal limits (Schoolfield & Sharpe, 1981; Angilletta, 2009; Hoffmann & Todgham, 2010; Schulte et al., 2011; Sunday et al., 2011; Diamond, 2017; Lancaster & Humphreys, 2020; Malusare et al., 2023; Briceño et al., 2025). Together these two facets of thermal biology (performance and tolerance) play a central role in shaping species distributions around the globe (Deutsch et al., 2008; Pörtner & Farrell, 2008; Kearney & Porter, 2009; Dell et al., 2011; Sunday et al., 2011; Kellermann et al., 2012; Bennett et al., 2021). Temperatures that support high performance, enabling growth, activity, and reproduction, influence where organisms can thrive, whereas the capacity to tolerate extreme temperatures constrains where they can persist. Because both performance and tolerance limits are known to correlate with geographic patterns of occurrence, changes in either dimension of the thermal environment can shift organisms' ranges (Pörtner & Farrell, 2008; Kearney & Porter, 2009; Dell et al., 2011; Kellermann et al., 2012; Lancaster & Humphreys, 2020; Bennett et al., 2021; Malusare et al., 2023; Briceño et al., 2025). As climate change drives increases in average temperatures and introduce greater thermal variability around the globe (IPCC, 2023), understanding how organisms respond to both conditions that support biological processes of life and conditions that exceed their tolerance limits and cause mortality is becoming increasingly urgent.

A number of classical and recent studies have emphasised how thermal traits representing either performance or tolerance are characterised by different thermal sensitivities and are likely governed by different biological processes (Angilletta, 2009; Ørsted et al., 2022; Buckley et al., 2022; Arnold et al., 2025). At intermediate and permissive temperatures, organisms can carry out essential

biological processes and maintain survival without acute stress (Ørsted et al., 2022). Within this permissive temperature range, or zone of resistance (Fry et al., 1946), performance traits are often represented by a nonlinear, bell-shaped thermal performance curve (TPC) (Fig. 1A). Performance in this thermal range is therefore typically assessed from traits that are considered supportive of fitness (i.e., growth or reproduction) to various extents. Heat stress incurred within this thermal range is manageable by homeostatic repair systems and thermal patterns of mortality are likely a result of thermal effects on senescence/aging rather than acute thermal stress (Pörtner & Farrell, 2008; Hoffmann & Todgham, 2010; Schulte, 2015; Ørsted et al., 2022). As temperatures become higher and more extreme the situation changes dramatically, with vastly different biological consequences. Exposure to stressful, high temperatures results in the disruption of essential biological processes and as a result survival is short and time limited (Collander, 1924; Alexandrov, 1964; Fry et al., 1946; Rezende et al., 2014; Jørgensen et al., 2019; Ørsted et al., 2022; Neuner & Buchner, 2023; Cook et al., 2024; Faber et al., 2024; Arnold et al., 2025). The intensity of thermal stress in this temperature range, referred to as the zone of tolerance (Fry et al., 1946), increases exponentially with temperature, such that log survival time decreases linearly, as described but the thermal death time (TDT) model (Bigelow, 1921; Fry et al., 1946; Rezende et al., 2014; Jørgensen et al., 2019; Faber et al., 2024). These stressful conditions are therefore disruptive, representing "negative" fitness outcomes as exposure to stressful temperatures leads to loss of homeostasis. Although the biological processes that support life, growth and reproduction at permissive temperatures differ and are antagonistic to those that lead to acute injury and failure at stressful temperatures, both are likely to influence species distributions in variable thermal environments (Ørsted et al., 2022; Arnold et al., 2025). Accordingly, organisms may be able to endure brief non-lethal exposure to stressful conditions, as long as they also have sufficient time to recover and regain performance under permissive temperatures. From this conceptual perspective, it is also clear that most measurements in thermal biology can be considered

146 correlates of either thermal performance or thermal tolerance. At the same time, it is equally evident
147 that the critical temperature (T_c) that separates the permissive vs. stressful thermal range, is central
148 for understanding thermal biology of ectotherms. Surprisingly, no assays that we are aware of are
149 designed specifically to characterise this transition temperature (or temperature zone) that is so central
150 for understanding and modelling the ectothermic response to thermal fluctuation.
151
152 In the present study we address this knowledge gab using two ectothermic organisms, one aquatic
153 plant (Gibbous duckweed, *Lemna gibba*) and one terrestrial animal (Spotted-winged drosophila,
154 *Drosophila suzukii*) to test four different methodological approaches to identify T_c, the temperature
155 (or temperature zone) that separates permissive and stressful temperatures. The first approach,
156 thermal performance assays (Fig. 1A), may provide an estimate of T_c when based on traits related to
157 fitness (e.g., reproduction), with the upper thermal limit of the performance curve approximating T_c
158 as the threshold beyond which organisms cannot maintain "positive fitness" and complete their
159 lifecycle (Huey & Kingsolver, 1989; Angilletta, 2009; Ørsted et al., 2022). In the second approach,
160 constant temperature assays (Fig. 1B), T_c corresponds to a breakpoint or change in linearity of $\log_{10}$
161 transformed time to thermal failure plotted against temperature. This approach rests on the
162 observation that the thermal sensitivity of lifespan is very different in the two thermal ranges since
163 the rate of aging/senescence (at permissive temperatures) typically has a Q_{10} of ~ 2 whereas or rate
164 of heat injury accumulation (at stressful temperatures) has a much higher thermal sensitivity Q_{10} >
165 1000 (Fig. 1B). The third approach, ramping assays (Fig. 1C-D), involves ramping assays initiated at
166 different starting temperatures but with a fixed ramping rate. When ramping begins at different
167 temperatures below T_c, it is expected that CT_{max} (i.e., the final temperature when the organism
168 succumbs to stress during the ramp) is similar as all treatment groups only start to accumulate damage
169 once they pass T_c. However, if the ramping assay is initiated at temperatures above T_c, then CT_{max}

should intuitively become higher since the exposed organisms have been "spared" from the injury that the other treatment groups accumulated between T_c and the higher start temperatures. T_c is thus inferred as the starting temperature at which the measured CT_{max} begins to increase (Fig. 1D). In the fourth approach we use alternating constant temperature assays (Fig. 1E-F). Here the organisms are first exposed to a stressful temperature for a set duration to induce sublethal damage (e.g., 50% of that causing failure) and then transferred to a lower "recovery" temperature before returning to the initial stressful temperature again until thermal failure is reached. This method identifies T_c from the "recovery" temperature threshold below which thermal damage does not accumulate, or below which recovery prolong the organism's tolerance to stress during the second stress exposure (Fig. 1F).

Following our experiments with the two model systems we evaluate these four methods with respect to their theoretical assumptions, practical implementation, and the extent to which they reflect the biological transition between permissive and stressful temperatures. For both model organisms, we find that three out of the four of methods converge on quantitatively similar estimates of T_c, while one method is found to be impractical and yields inaccurate estimates for both species. Using these observations, we provide both a philosophical and practical guidance on how to assess T_c in ectotherms and highlight how this parameter should be considered as an important thermal parameter in consideration of global warming impacts on ectothermic organisms.

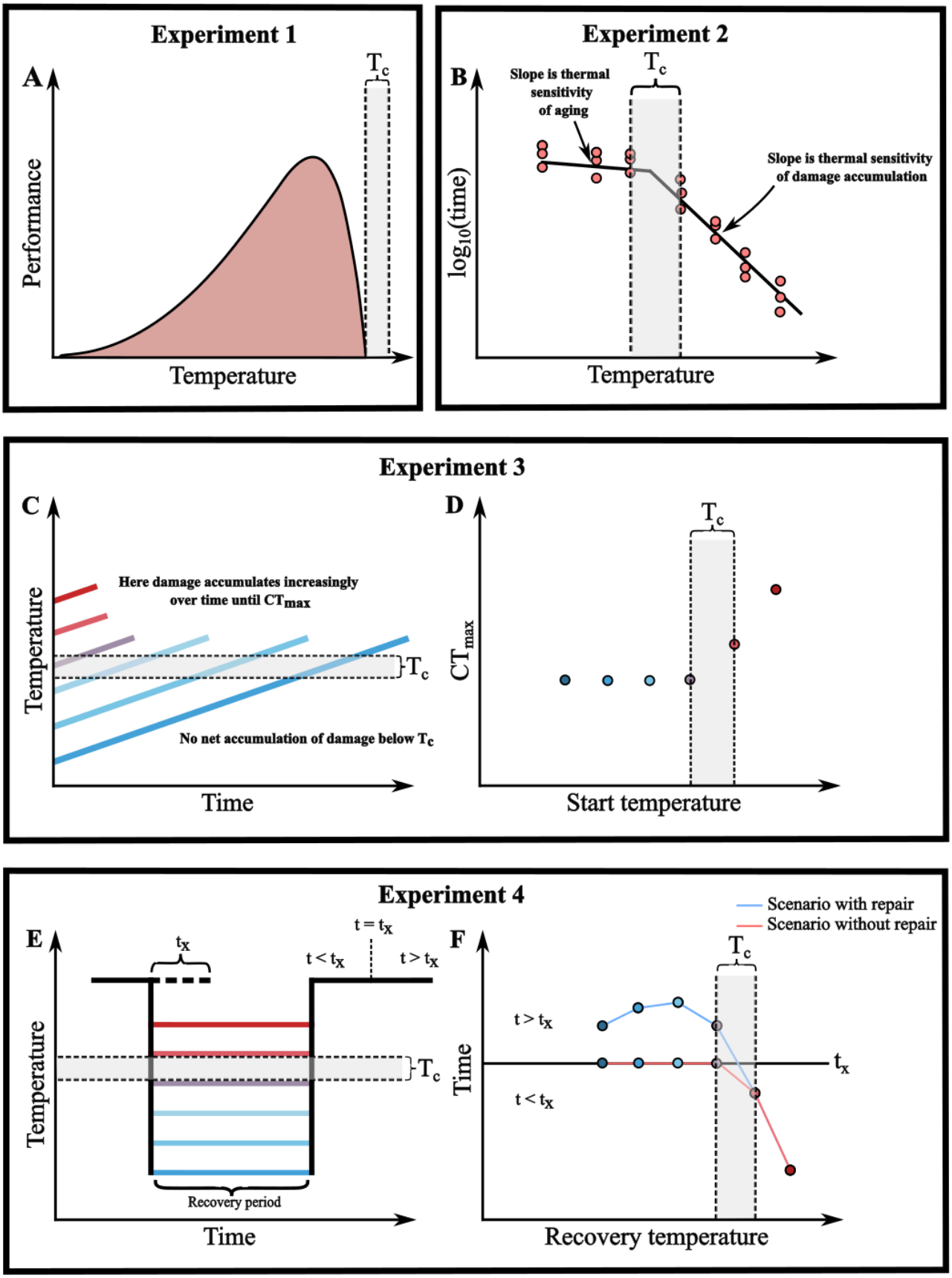
Experiment 1
A
Performance
Temperature
T_c
Experiment 2
B
Slope is thermal sensitivity of aging
Slope is thermal sensitivity of damage accumulation
$\log_{10}$(time)
Temperature
T_c
Experiment 3
C
Here damage accumulates increasingly over time until CT_{max}
No net accumulation of damage below T_c
Temperature
Time
T_c
D
CT_{max}
Start temperature
T_c
Experiment 4
E
t_x
$t = t_x$
$t < t_x$
$t > t_x$
Recovery period
Temperature
Time
T_c
F
Scenario with repair
Scenario without repair
T_c
$t > t_x$
$t < t_x$
t_x
Time
Recovery temperature

189

Figure 1. Conceptual approaches for identifying the critical temperature (T_c), represented as a narrow range of temperatures (red area between the two dotted lines in each graph), using thermal performance assays in experiment 1 (**A**), constant temperature assays in experiment 2 (**B**), ramping assays in experiment 3 (**C** and **D**) and alternating constant temperature assays in experiment 4 (**E** and **F**). **A** illustrates how thermal performance assays when based on fitness related traits (e.g., growth/reproduction) may provide an estimate of T_c, where the upper thermal limit of the performance measure represents a temperature approaching T_c (i.e. beyond T_c organisms cannot maintain net positive fitness). **B** depicts how constant temperature assays, where a breakpoint of a change in linearity of $\log_{10}$ transformed time to thermal failure plotted against temperature corresponds to T_c. This assay exploits that the thermal sensitivity (slope of the temperature response) of aging and injury are dramatically different with a hypothetical breakpoint at Tc. **C** and **D** depict how ramping temperature assays initiated at different starting temperatures but with a constant ramping rate can reveal the temperatures resulting in thermal damage accumulation and thus identify T_c. **C**) Temperature profiles for each assay, with temperature (°C) on the y-axis and time (minutes) on the x-axis. **D**) Corresponding CT_{max} estimates for each temperature profile, with the y-axis showing CT_{max} and the x-axis showing the ramping assay's starting temperature. If ramps begin below T_c, CT_{max} estimates remain stable: if ramps begin above T_c, CT_{max} increases, as part of the stressful damaging temperature range is bypassed. **E** and **F** illustrate how alternating constant temperature assays can be used to identify the temperatures resulting in accumulation of thermal damage and thus identify T_c. In this approach, organisms are first exposed to a stressful temperature for a duration sufficient to induce a non-lethal dose of damage (e.g. 50% damage). After this initial exposure, the temperature is lowered to a recovery temperature for a defined period before the organisms are returned to the original stressful temperature until thermal failure is observed. If the initial exposure induces 50% damage, organisms should succumb after experiencing the remaining 50% exposure duration at the second exposure. However, if repair occurs during the recovery period then the time to failure will be extended in the second round. Thus, after the recovery phase, organisms will fail at the same additional exposure duration (t_x) if the recovery temperature does not extend survival time, whereas failure will occur later than t_x ($t > t_x$) if the recovery temperature allows repair of accumulated damage, thereby extending survival time. **E** depicts the temperature profiles for these assays, with temperature on the y-axis and time on the x-axis. **F** shows the resulting time to thermal failure plotted against recovery temperature, illustrating how different recovery temperatures either maintain, increase or reduce accumulated damage.

Materials and methods

Growth and rearing conditions

A stock culture of *L. gibba* was maintained at ~21 °C in continuous light in a plastic container (~30 × 50 cm) filled with 3 L of demineralized water supplemented with 2 g L^{-1} of Schenk & Hildebrandt basal salt medium (Duchefa biochemie, Haarlem, Netherlands). Water and salt medium was renewed twice per week to maintain nutrient availability and water quality. The water was constantly aerated to ensure oxygenation and prevent stagnant water. Photosynthetic photon flux density (PPFD) at the level of the plants was kept at ~150 µmol m^{-2} s^{-1}, using full-spectrum LED lamps. Excess duckweed was continuously removed from the culture to ensure optimal population density for healthy and uniform plant development.

D. suzukii were maintained in a temperature-controlled room at 19 °C under a 22:2 h light:dark cycle. For fly rearing ~200 parental flies were placed in 350 ml Drosophila culture flasks containing 40 ml of oat-based nutrient medium (ingredients per liter water: 60 g yeast, 40 g sucrose, 30 g oatmeal, 16 g agar, 12 g methylparaben (Nipagen), and 1.2 mL acetic acid). The parental flies were moved to fresh culture flasks once a week and a piece of paper was inserted into the medium in each flask to provide a suitable pupation surface for the emerging larvae. To synchronize age of experimental flies the emerging flies were collected every 2-3 days and then rapidly sexed under brief CO_2 anaesthesia (<5 minutes). The male and female flies were subsequently maintained in 30 mL vials with 5 mL food with ~50 flies per vial. All flies were allowed to recover for a minimum of three days following CO_2 exposure before they were used in experiments.

Assessment of thermal failure

Thermal failure was defined differently for each species. For *L. gibba* the thermal endpoint was estimated from loss of photosynthetic function. Thus, acute thermal failure of *L. gibb*a was defined as a 50% decrease in the maximum quantum efficiency of photosystem II (F_v/F_m) measured using a FluorPen FP 110 (Photon systems instruments, Czech Republic). Here F_v and F_m represent the variable and maximum fluorescence, respectively, measured on dark-adapted fronds, where F_v is calculated as the difference between the dark-adapted maximum and minimum fluorescence (F_0). A reduction in F_v/F_m of ~50% indicates significant dysfunction of the photosynthetic apparatus and visible tissue-level damage (Schreiber & Berry, 1977; Downton & Berry, 1982; Berry & Bjorkman, 1980; Knight & Ackerly, 2003; Sastry & Barua, 2017).

For *D. suzukii* the thermal endpoint was measured from the entry of heat coma which is registered as the time/temperature at which individuals show no movement in response to tapping and shaking of their container. The entry into heat coma occurs slightly before heat mortality so heat coma is not a direct measure of survival even if the relation between heat coma and heat mortality is strong in drosophila including *D. suzukii* (Jørgensen et al., 2020 and Ørsted et al., 2024). In the present study the species-specific thermal endpoints were applied across all acute thermal failure experiments (i.e., constant temperature assays, ramping temperature assays with different starting temperatures, and alternating constant temperature assays).

Acute thermal stress protocol for *Lemna gibba*

In all experiments for estimation of acute thermal failure for *L. gibba*, we used a standardized thermal stress protocol following a similar methodology to Faber et al., 2024. For each treatment, individual plants were randomly selected from the stock culture and transferred to transparent 50 ml Greiner

tubes (~50 individuals pr. tube) containing 15 ml of demineralized water supplemented with Schenk & Hildebrandt basal salt medium (2 g L^{-1}; Duchefa Biochemie, Haarlem, Netherlands). The tubes were then sealed and placed horizontally in temperature-controlled water baths. During heat exposure, the samples were illuminated from above at ~150 µmol m^{-2} s^{-1} PPFD to simulate the same light conditions as in the stock culture. Exposure duration was varied across replicate tubes by removing them at regular time intervals throughout the stress treatments. This was done to generate time-response curves for each treatment allowing the estimation of when F_v/F_m decreased with 50%, defined as thermal failure (see below). After treatment, all tubes were filled with tap water (~20-21 °C) to reduce the plants tissue temperature immediately after stress and placed in darkness at ~21 °C for 24 hours to allow damage to accumulate. Following this period, maximum quantum efficiency of PSII (F_v/F_m) was measured on 30 randomly selected individuals per tube to assess thermal tolerance.

Estimating thermal failure for *L. gibba*

Thermal failure was estimated for *L. gibba* in the constant temperature (Fig S1), ramping temperature (Fig S2) and alternating constant temperature (Fig. S3) assays using generalized additive models (GAMs). GAMs were used to estimate the decrease in F_V/F_M following the stress treatments and determine the time point or temperature at which a lethal dose of damage to PSII occurred (i.e., when F_V/F_M decreased by 50% according to the fitted GAMs). GAMs were fitted to F_V/F_M measurements as a function of stress duration, using automated smoothness selection in the *mgcv* library in R and restricted maximum likelihood (REML) (Wood, 2017). The GAMs had the following components:

$$y_i = \alpha + f(x_i) + \varepsilon_i \qquad \text{(Eqn. 1)}$$

290 Where y_i is the observation at time x_i, α is the intercept, $f(x_i)$ is a smooth function and ε_i is the
291 residual error. This approach makes no *a priori* assumption about the functional relationship between
292 variables (Wood, 2017), allowing a non-parametric depiction of the empirical trend of the response
293 over time.
294
295 **Experiment 1: thermal performance assays**
296 Thermal performance assays may provide an estimate of T_c when based on traits related to fitness
297 (e.g., reproduction), with the upper thermal limit of the performance curve approximating T_c as the
298 threshold beyond which organisms cannot complete their lifecycle (Fig. 1A) (Ørsted et al., 2022). To
299 evaluate thermal performance in relation to reproductive success and development, *L. gibba* and *D.*
300 *suzukii* were exposed to a range of constant, permissive temperatures either approaching or
301 overlapping into the estimated stressful temperature range. Based on clonal reproduction in *L.*
302 *gibba* and on pupal development, hatching success, and adult survival in *D. suzukii*, T_c was estimated
303 in these thermal performance assays as the lowest temperature at which the performance of these
304 traits approached zero.
305
306 For *L. gibba*, individuals were randomly selected from the stock culture, excluding those visibly
307 undergoing clonal division. For each temperature treatment, five replicate Greiner tubes were
308 prepared, with five randomly selected individuals assigned to each tube. The tubes were submerged
309 in temperature-controlled water baths set at 25, 30, 35, 38, 39, or 40 °C and maintained under
310 continuous light at ~150 µmol m^{-2} s^{-1} PPFD to match the light conditions in the stock culture. After
311 72 hours of continuous exposure, the number of living and dead individuals in each tube was
312 recorded. Individuals were considered dead when tissues showed complete whitening.
313

For *D. suzukii*, adult males and females were combined within the same vial for each temperature treatment. Ten replicate vials were prepared per temperature, each containing 10 males and 10 females. The vials were placed at 27, 28, 29, 30, or 31 °C and maintained for 96 hours to allow mating and egg laying. After 96 hours, adult survival was assessed for both sexes in each vial, after which all adult flies (dead or alive) were removed. The vials were then returned to their designated temperatures to allow development of eggs and larvae. Each vial was monitored in the subsequent 21 days for larval activity, and number of pupae and newly emerged adults were recorded.

Experiment 2: constant temperature assays

To assess thermal tolerance across a range of constant temperatures and generate TDT models, replicate batches of individuals from both *L. gibba* and *D. suzukii* were exposed to heat stress at a range of fixed temperatures until acute thermal failure was reached (see below for details). To estimate T_c from these assays, a piecewise linear regression analysis was applied using the segmented package (Muggeo, 2008) in R v.4.1.0 (R Core Team, 2021) to detect breakpoints in the relationship between the $\log_{10}$-transformed time to thermal failure and temperature for each species (Fig. 1B). The fit of the segmented model was compared to a linear regression using an F-test to determine whether the breakpoint was significant. TDT models were generated for each species by fitting linear regressions to the $\log_{10}$-transformed time to thermal failure plotted against temperature, using data above the estimated T_c. The slopes of the TDT models were used to calculate Q_{10} values, which represent the fold-change in mortality rate per 10 °C increase. The Q_{10} values were used to quantify the temperature-dependence and sensitivity of the rate of thermal failure above T_c.

For *L. gibba*, replicate Greiner tubes containing ~50 individuals were prepared and treated according to the acute thermal stress protocol for *L. gibba* (see above). Accordingly, sealed tubes were

submerged horizontally in temperature-controlled water baths set at constant temperatures ranging from 36 °C to 44 °C in 1 °C increments. For each temperature, replicate tubes were removed at different exposure durations and subsequently exposed to a 24-hour dark period at ~21 °C. Thermal damage was then quantified by measuring F_v/F_m on 30 randomly selected individuals from each tube. For treatments with exposure durations longer than four days, the water solution in the tubes were renewed every 5th day to maintain nutrient availability throughout the experiment.

For *D. suzukii*, adult flies were exposed to constant temperatures of 19 °C, and from 25 °C to 37 °C in 1 °C increments. At each temperature, groups of 10 flies were placed in 5 mL glass vials containing a small amount of food. For temperatures of 33 °C and above, vials were sealed and submerged in water baths. For temperatures of 32 °C and below, vials were placed in temperature-controlled incubators such that the flies had access to fresh air. The flies were observed until coma occurred, with observations made at regular intervals depending on the expected time to coma. These data were used to calculate Lt_{50} at each temperature, defined as the time at which 50% of all flies had reached coma.

Experiment 3: ramping temperature assays with different starting temperatures

For estimating T_c with ramping assays, both *L. gibba* and *D. suzukii* were exposed to temperature ramps with fixed ramp rates starting from different initial temperatures (Fig. 1 C-D). For these assays, when ramps are initiated at temperatures below T_c, organisms are expected to accumulate damage similarly across treatments, resulting in consistent CT_{max} values (i.e., the temperature at which thermal failure occurs during the ramp). However, when the assays are initiated at temperatures above T_c, a portion of the stressful temperature range is bypassed. As a result, the ramps must increase further to higher temperatures for the organisms to accumulate a lethal dose of damage, leading to

362 elevated CT_{max} values (Fig. 1D). To estimate T_c from these assays, piecewise linear regressions were
363 applied to detect breakpoints in the relationship between CT_{max} and the starting temperatures of the
364 ramps and compared to linear regression models fitted to the same data with an F-test to test whether
365 the breakpoints were significant. The breakpoints were interpreted as T_c, marking the starting
366 temperature in the assays above which CT_{max} begins to increase and the transition between the
367 permissive and stressful temperature range.
368
369 For *L. gibba*, replicate Greiner tubes containing ~50 individuals were prepared following the acute
370 thermal stress protocol for *L. gibba* (see above). The tubes were then horizontally submerged in water
371 baths starting at 26 °C, 30 °C, 34 °C, 38 °C, or 42 °C. From each starting temperature, the bath
372 temperature was increased at a constant rate of 0.15 °C per minute. At predetermined time points
373 during the ramp, tubes were removed and transferred to darkness at ~21 °C for 24 hours to allow
374 damage to accumulate before thermal tolerance was assessed by measuring F_v/F_m on 30 randomly
375 selected individuals from each tube.
376
377 For *D. suzukii*, groups of 12 individuals were sealed in 5 mL glass vials with a small food source.
378 Each group was exposed to a temperature ramp in a water bath that began at one of several starting
379 temperatures between 25 and 39 °C, in 1 °C increments. The temperature in the water bath was
380 subsequently increased at a constant rate of 0.1 °C per minute. The flies were continuously monitored
381 during heating, and the temperature at which each individual reached coma was recorded.
382
383 **Experiment 4: Alternating constant temperature assays**
384 For the alternating constant temperature assays, *L. gibba* and *D. suzukii* were initially exposed to a
385 constant stressful temperature (*L. gibba*: 43 °C and *D. suzukii*: 35.2 °C) for a duration corresponding

386 to approximately 50% of a lethal dose (50% of Lt_{50}) of thermal damage. The exact temperature used
387 was either calculated using the TDT model derived from the constant temperature assays (*L. gibba*)
388 validated directly a "control" to determine Lt50 at this temperature (*D. suzukii*). They were then
389 transferred to lower "recovery" temperatures for either six hours (*L. gibba*) or four hours (*D. suzukii*),
390 followed by re-exposure to the initial stressful temperature (Fig. 1E). For these assays, T_c can be
391 estimated as the "recovery" temperature at which damage begins to accumulate. When the
392 temperature drop is below T_c during "recovery", damage accumulation should pause or potentially
393 allowing repair of previous damage accumulation and this should prolong or maintain survival time
394 during the second heat stress exposure. However, if the "recovery" temperature drop is above T_c,
395 damage should continue to accumulate during "recovery", and the survival time during the second
396 heat stress exposure should be shorter (Fig. 1E, F). To identify this threshold, observed survival times
397 across all assays were compared to the expected survival time. The expected survival time at the
398 initial stressful temperature represents the expected survival duration if no damage accumulated
399 during the recovery period as illustrated as time t_x in Fig. 1E, F. If the observed survival time is
400 markedly shorter than this value ($t < t_x$), the temperature is above T_c, whereas when the observed
401 survival time is markedly longer than t_x ($t > t_x$) the temperature is below T_c.
402
403 For *L. gibba*, replicate tubes were prepared according to the acute thermal stress protocol for *L. gibba*
404 (see above). The tubes were first exposed to a constant high temperature of 43 °C for 41 minutes,
405 corresponding to the estimated 50% lethal dose of damage based on the TDT model. The tubes were
406 then transferred to one of seven lower recovery temperatures (26, 30, 34, 36, 38, 40, or 42 °C) for six
407 hours before being returned to 43 °C. After treatment, the tubes were placed in darkness at ~21 °C for
408 24 hours before measuring F_v/F_m on 30 randomly selected individuals. T_c was estimated by
409 comparing the observed survival time in each assay relative to the expected survival time at 43 °C

410 (i.e., ~82 minutes). As no recovery or hardening was observed for any of the assays that could extend
411 survival time beyond t_x ($t > t_x$), T_c was estimated using a piecewise linear regression analysis to
412 identify the breakpoint at which time to thermal failure began to decrease with recovery temperature
413 relative to the expected survival time at 43 °C (see example without recovery in Fig. 1F).
414
415 For *D. suzukii*, eight groups of ten flies (each females placed in a 5 ml vial) were first exposed to
416 35.2 °C in a water bath for 90 minutes, corresponding to a 50% lethal dose of damage. One control
417 group remained in the water bath, to verify that heat coma occurred around 3 hours of exposure. The
418 other seven groups were moved to thermal incubators set at recovery temperatures of 28, 29, 30, 31,
419 32, 33, or 34 °C for four hours after which all groups were returned to 35.2 °C in the water bath.
420 These flies were monitored continuously until time of coma. Hardening and/or repair did extend
421 survival time beyond t_x ($t > t_x$) for some assays (see example with recovery in Fig. 1F). As a result,
422 T_c was estimated by comparing differences in survival times between the assays and the control group
423 using a t-test with Benjamini-Hochberg correction for multiple comparisons to determine the
424 temperature at which time to thermal failure began to decline significantly the expected survival time
425 at 35.2 °C. The black silhouette images in of *L. gibba* and *D. suzukii* images were obtained from the
426 PhyloPic database; created by Guillaume Dera (*L. gibba*) and Nicolas Gompel (*D. suzukii*) (CC0 1.0)
427
428 **Results**
429 **Estimating T_c from thermal performance assays**
430 To estimate T_c using thermal performance assays, *L. gibba* and *D. suzukii* were exposed to a range of
431 constant temperatures: *L. gibba* was exposed to temperatures from 25 to 40 °C for 78 hours and *D.*
432 *suzukii* from 27 to 31°C for 96 hours. For *L. gibba*, the net population change (increase or decrease
433 in number of alive individuals) were measured following each temperature treatment. For *D. suzukii*,

adult flies were exposed to the temperature treatments to assess their survival and the resulting pupal and adult emergence at each temperature.

For *L. gibba*, net population change declined progressively from 25 °C to 40 °C (Fig. 2). At temperatures up to 37 °C, population size increased, indicating that reproduction exceeded mortality. At 38 °C and above, population change approached zero or became negative, reflecting minimal reproduction and rising mortality, with 100% mortality occurring at 40 °C. These results indicate that reproduction was substantially reduced near 38 °C, while rates increased beyond this point. Together, these patterns suggest that T_c lies close to 38 °C.

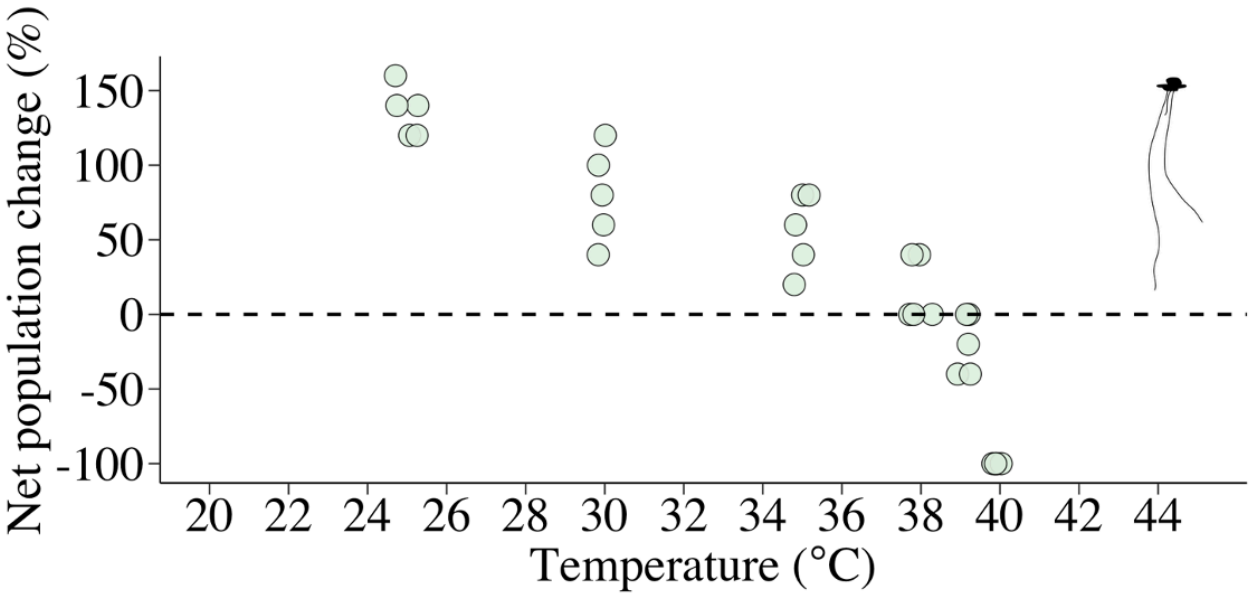

Figure 2. Net population change of *Lemna gibba* after 72 hours of exposure at different constant temperatures. Each point represents the outcome following the 72 hours of exposure from one of five replicates (starting with 5 individuals per replicate) at a given temperature (°C) depicted on the x-axis with random jitter added to the datapoints. The y-axis shows the net change in population size, with circles above 0 indicating net reproduction and circles below 0 indicating net mortality. The net population change (%) represents the percent change in the number of living individuals relative to the initial population (5 individuals per replicate), calculated as (((final number of individuals)-5)/5)×100.

For *D. suzukii*, the mean number of parental flies surviving the 4 day egg laying period began to decrease at 29 °C and at 31 °C all individuals were dead after 96 hours (Fig. 3A). We observed larval activity in almost all the food vials between 27 °C and 30 °C but no activity at 31 °C (Fig. 3B). The number of pupae developing from the larvae decreased progressively from 27 °C and no pupae emerged from the developmental temperature of 31 °C (Fig. 3C). Likewise, the number of adults offspring emerging from pupae declined sharply above 27 °C and no adult offspring emerged at temperatures from 29 °C or above (Fig. 3B). These results suggest that T_c for development in *D. suzukii* is between 29 °C and 31 °C and for all stages of development to succeed a temperature below 29 °C is needed.

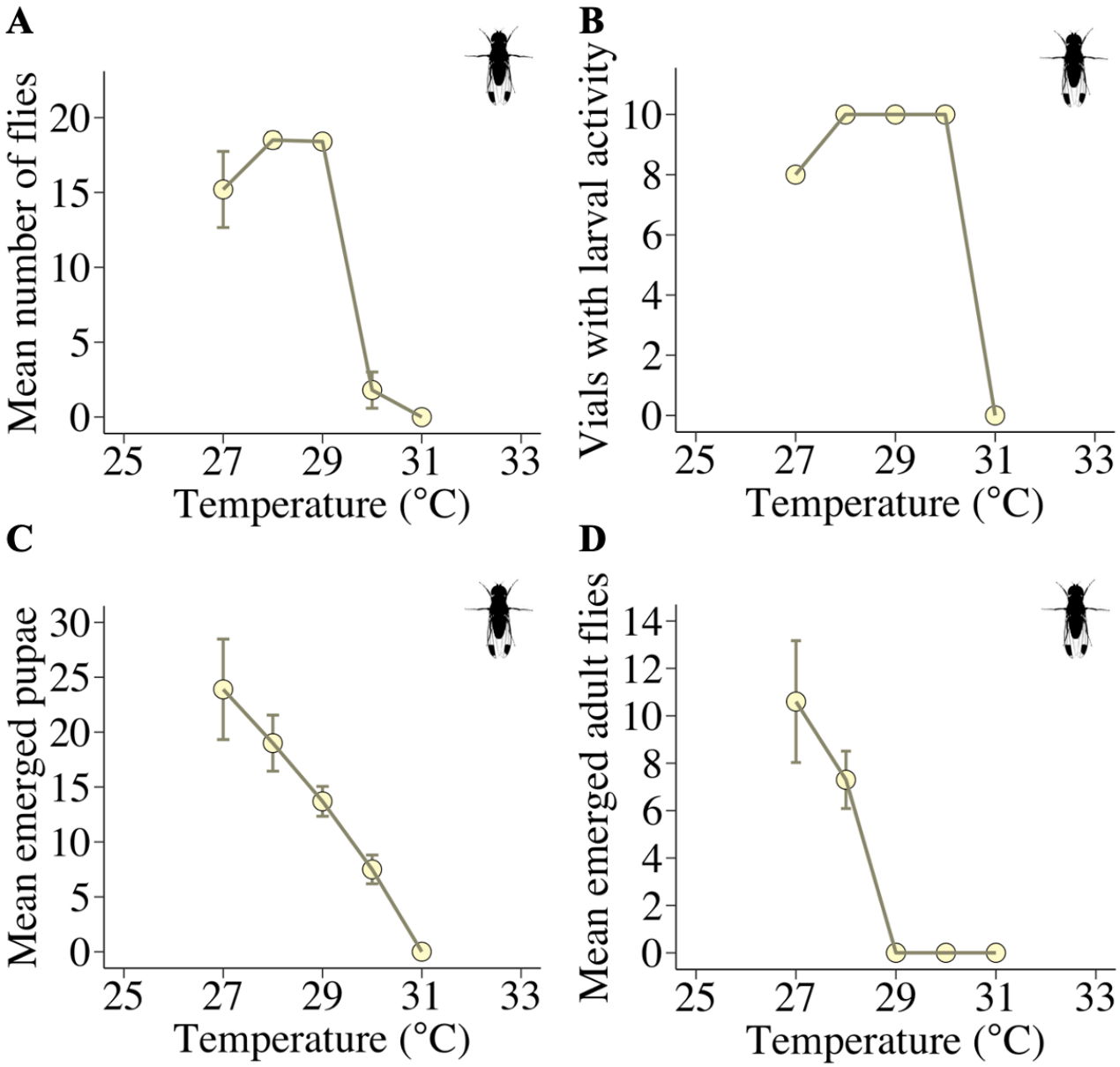

Figure 3. Thermal performance of *Drosophila suzukii* across different constant temperatures (27 °C to 31 °C) depicted on the x-axis, measured through sequential developmental stages. Adult flies (10 vials per temperature, 10 males and 10 females per vial) were exposed to each temperature for 96 hours to allow mating and oviposition. A) Mean number of living adult flies per vial after 96 hours of exposure. B) Number of vials with larval activity observed within 21 days following removal of adults from the vials. C) Mean number of pupae that developed from the eggs laid during the exposure period. D) Mean number of adult flies that successfully emerged from those pupae. Error bars represent the standard error of the mean.

Estimating T_c with constant temperature assays

To estimate T_c from constant temperature assays, we analysed the relationship between the $\log_{10}$-transformed time to thermal failure and temperature, identifying T_c as breakpoints, beyond which mortality rates increased significantly. For both *L. gibba* and *D. suzukii*, the time to thermal failure decreased exponentially with the intensity of the temperature stress (Fig. 4A,B).

For *L. gibba*, the time for F_v/F_m to decline with 50%, decreased exponentially from 38 to 44 °C. This relationship was well described by a TDT model, based on the linear relationship between the $\log_{10}$-transformed time to thermal failure and temperature ($R^2 = 0.98$, $P < 0.05$) (Fig. 4A). The Q_{10} value calculated over this temperature range was 25044, indicating a high thermal sensitivity. A piecewise linear regression revealed a breakpoint at 38 °C ± 0.697 SE, with this model providing a significantly better fit than a simple linear model ($P < 0.05$). Below this breakpoint, thermal sensitivity was reduced, as reflected by a lower Q_{10} of 33.65. This suggests a T_c of approximately 38 °C for *L. gibba.*

Similarly, *D. suzukii* displayed an exponential decrease in time to thermal failure over the temperature range of 27 to 37 °C. The relationship between $\log_{10}$-transformed time to failure and temperature was also well described by a TDT model ($R^2 = 0.97$, $P < 0.05$) (Fig. 4B). The Q_{10} value for this range was 6754.97, indicating a high thermal sensitivity. A breakpoint was detected at 27.15 °C ± 0.60 SE, with piecewise regression significantly improving model fit compared to a linear model ($P < 0.05$). Below this threshold, the Q_{10} dropped to 0.89, indicating a marked reduction in thermal sensitivity. This supports a T_c value of 27.15 °C for *D. suzukii*.

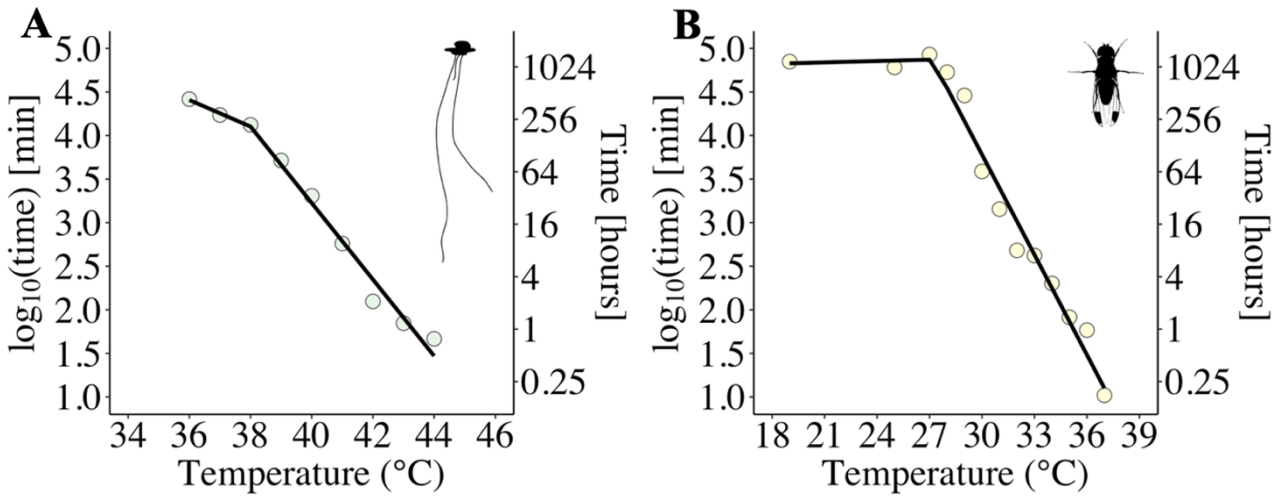

Figure 4. Thermal death time (TDT) models for A) *Lemna gibba* and B) *Drosophila suzukii* based on a range of constant temperature exposures. The y-axis shows the $\log_{10}$-transformed time (minutes) until thermal failure, the secondary y-axis shows the time to thermal failure in hours, and the x-axis shows the temperature (°C) of each thermal stress treatment. For *L. gibba*, thermal failure was defined as the time when F_v/F_m decreased with 50 %, while for *D. suzukii*, it was defined as the mean time at which individuals reached comatose. Piecewise linear regression models (black lines) revealed breakpoints at 38 °C ± 0.697 SE for *L. gibba* and 27.15 °C ± 0.60 SE for *D. suzukii*, and linear sections above these breakpoints representing the TDT models.

Estimating T_c from ramping temperature assays with different starting temperatures

For estimating T_c from ramping assays with different starting temperatures, CT_{max} was measured for *L. gibba* and *D. suzukii* across a series of ramping assays initiated at different temperatures with a fixed ramp rate (*L. gibba*: 0.15 °C/min, *D. suzukii*: 0.344 °C/min). A piecewise linear regression analysis was used to identify the starting temperature at which CT_{max} began to increase, indicating the threshold (T_c) above which thermal damage began to accumulate.

For *L. gibba*, CT_{max} remained unchanged at an average of 45.69 °C ± 0.23 SE across all starting temperatures from 26 to 42 °C (Fig. 5), and as indicated by the piecewise linear regression, which did not identify a significant breakpoint or improve fit over a linear model ($P > 0.05$) (Fig. 5A). This suggests that damage accumulation did not contribute considerably to the total "stress dose" at the

lower end of the stressful temperature range, even though the some experiments included damage accumulation in the range of 38 to 42 °C and others did not.

A similar pattern was observed for *D. suzukii*, where the average CT_{max} estimate remained consistent around 36.8 °C ± 0.11 SE across starting temperatures from 25 to 36 °C (Fig. 5B). CT_{max} increased slowly at lower starting temperatures but only began to substantially increase when ramping was initiated at 36 °C or above, indicating that the contribution of injury accumulated at the lower stressful temperature range of this assay is negliable (Fig. 5B**)**. A piecewise linear regression supported this with identifying a significant breakpoint at 36.51 °C ± 0.34 SE and improved fit over a linear model ($P < 0.05$) (Fig. 5B).

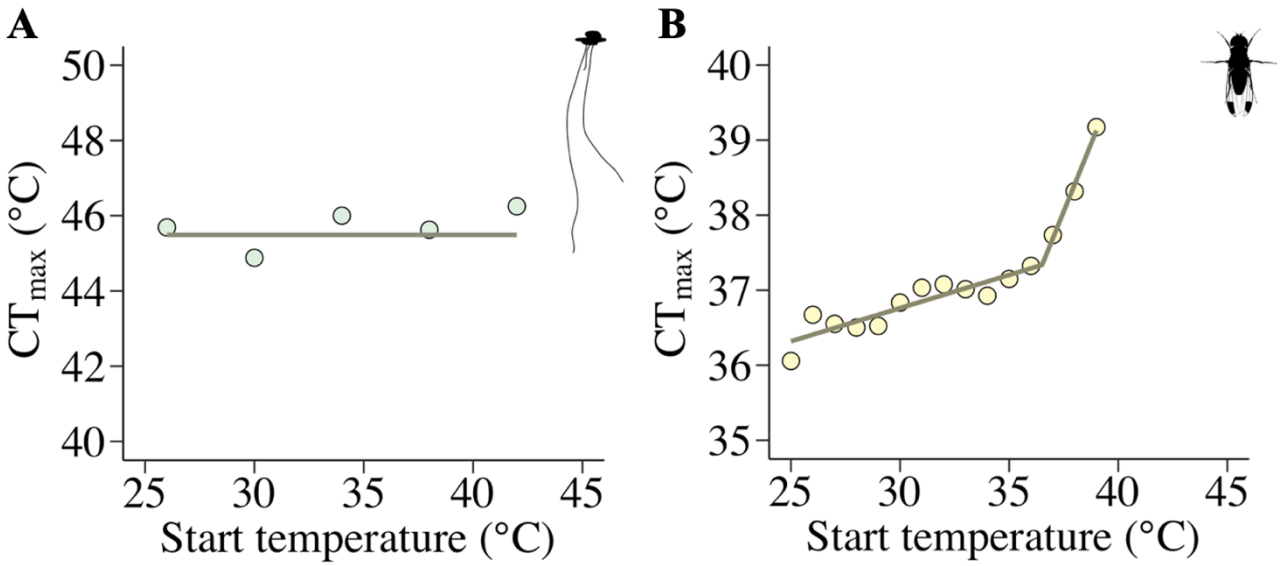

Figure 5. CT_{max} for *Lemna gibba* (A) and *Drosophila suzukii* (B) across a series of ramping assays initiated at different temperatures with a fixed ramp rate (*L. gibba*: 0.15 °C/min, *D. suzukii*: 0.344 °C/min). The y-axis depicts CT_{max} (green circles for *L. gibba*, yellow circles for *D. suzukii*), and the x-axis shows the temperature (°C) that each ramping assay was initiated at. For *L. gibba*, thermal failure was defined as the time when F_v/F_m decreased with 50%, whereas for *D. suzukii*, it was defined as the mean time at which the flies reached comatose. Piecewise linear regression models were used to assess whether CT_{max} changed with different starting temperatures for the ramping assays. The best-fitting model was selected based on an F-test, with the piecewise model shown in panel B and a linear regression model shown in panel A.

528 **Estimating T_c from assays with alternating constant temperatures**

529 To estimate T_c under alternating constant temperature assays, *L. gibba* and *D. suzukii* were initially
530 exposed to constant stressful temperatures for durations resulting in approximately 50% of the time
531 needed to reach Lt_{50} (*L. gibba*: 43 °C and *D. suzukii*: 35.2 °C). The organisms were then exposed to
532 a "recovery" temperature, by being transferred to lower temperatures for either six (*L. gibba*) or four
533 (*D. suzukii*) hours, followed by a return to their initial stressful temperature treatment where they
534 were observed until thermal failure. The expected time to thermal failure under uninterrupted
535 exposure to the initial stress temperature is denoted as t_x and serves as a control, representing the
536 survival time if no recovery period had occurred.

537

538 For *L. gibba*, exposure to recovery temperature between 26 and 38 °C resulted in times to thermal
539 failure that were similar to t_x, indicating that interrupting exposure to 43 °C with these recovery
540 temperatures neither alleviated nor exacerbated thermal damage (Fig. 6A). In contrast, "recovery"
541 temperatures above 38 °C reduced time to thermal failure relative to t_x, demonstrating that these
542 higher "recovery" temperatures caused additional damage rather than enabling recovery (Fig. 6A).
543 This was supported by a piecewise linear regression analysis, which identified a significant
544 breakpoint at 39.70 °C ± 0.13 SE and showed improved model fit over a linear model ($P < 0.05$). This
545 increase in damage accumulation beyond the breakpoint indicates T_c for *L. gibba*, as it marks the
546 threshold beyond which damage accumulation begins to increase.

547

548 For *D. suzukii*, the time to thermal failure was significantly longer than t_x when the recovery
549 temperatures ranged from 28 °C to 31 °C, indicating that exposure to these recovery temperatures
550 resulted in net repair relative to uninterrupted exposure to the initial stress temperature of 35.2 °C
551 (Fig. 6B). At recovery temperatures of 32 °C time to thermal failure did not differ significantly from

552 t_x (Fig. 6B) indicating that this "recovery" temperatures did not support recovery and using a recovery
553 temperature of 33 °C resulted in a tolerance time of less than t_x (although not significantly) suggesting
554 that "recovery" above 32 °C are above T_c for *D. suzukii*.

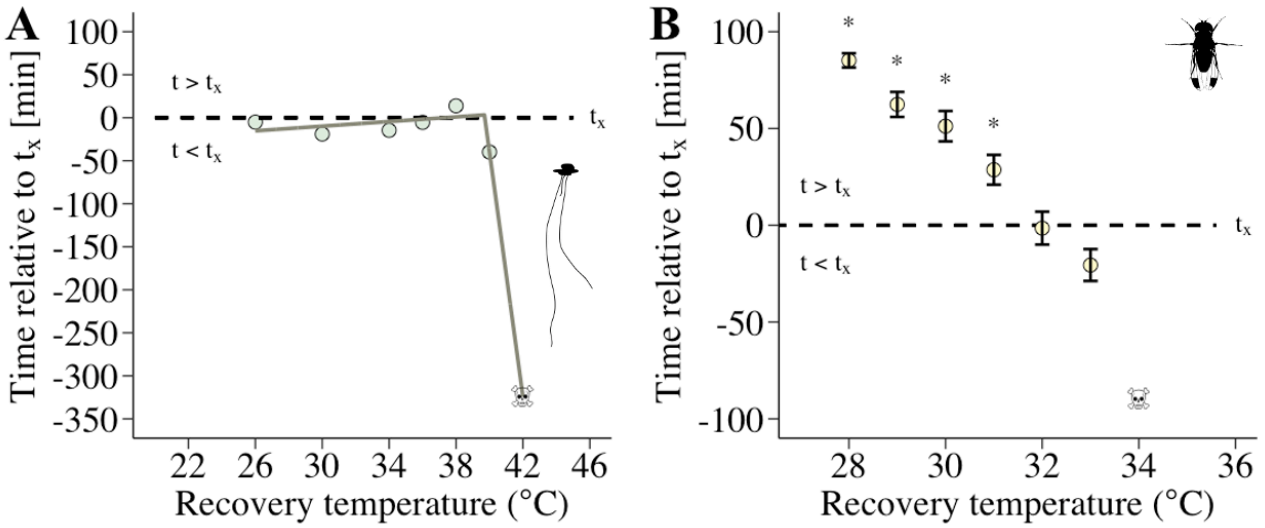

555

556 **Figure 6.** Time to thermal failure of *Lemna gibba* (A) and *Drosophila suzukii* (B) under alternating constant temperature
557 assays. Individuals of both species were initially exposed to a stressful temperature that causes approximately 50%
558 damage (L. gibba: 43 °C; D. suzukii: 35.2 °C). They were then transferred to a lower "recovery" temperature for a fixed
559 period (L. gibba: 25-42 °C for six hours; D. suzukii: 26-31 °C for four hours), before being returned to the initial stress
560 temperature until thermal failure occurred, if not already reached. The y-axis shows the time to thermal failure relative to
561 t_x, where t_x is the expected time to thermal failure if the recovery temperatures caused no additional damage or increase
562 lifespan. The dotted lines represent t_x. Values above the line ($t > t_x$) indicate that recovery temperatures slowed thermal
563 damage relative to t_x, whereas values below the line ($t < t_x$) indicate that recovery temperatures caused additional damage,
564 accelerating thermal failure. The x-axis shows the different recovery temperatures (°C) used in the assays. For *L. gibba*,
565 thermal failure was defined as the time when F_v/F_m decreased with 50%, whereas for *D. suzukii*, it was defined as the
566 time at which the flies reached comatose. A skull symbol at 42 °C (panel A) and 34 °C (panel B) indicates that the
567 organisms reached thermal failure during the recovery period (for the flies this time was unspecified). Asterisks in B)
568 indicate recovery temperatures at which the time to thermal failure for *D. suzukii* was significantly different from t_x, as
569 determined by a two-sample t-test with Benjamini-Hochberg correction for multiple comparisons ($P < 0.05$).
570
571

Discussion

T_c as a transition between performance and acute failure

Data from several experiments and in two different model systems supports the idea that T_c represents a fundamental biological threshold that that characterises the thermal boundary between temperatures that allow sustained biological function and temperatures that cause consistent and often rapid loss of loss of homeostasis. Conceptually, this transition aligns with long-standing distinctions in thermal biology between permissive and stressful temperatures, historically described as the zone of resistance and the zone of tolerance, respectively (e.g. Alexandrov, 1964; Levitt, 1980; Cossins & Bowler, 1987). Within the zone of resistance, organisms can maintain homeostasis, such that physiological damage incurred at elevated temperatures can be counterbalanced by repair and regulatory processes. In contrast, temperatures within the zone of tolerance impose stress levels that overwhelm these mechanisms, leading to the accumulation of damage and sharply reduced survival times. In this framework, T_c can be viewed as the temperature (or narrow zone of temperatures) at which the balance between the rate of homeostatic maintenance and the rate of homeostatic disruption are equal (Ørsted et al., 2022). Across the two phylogenetically and ecologically distinct ectotherms in this study, the aquatic plant *L. gibba* and the fruit fly *D. suzukii*, T_c consistently emerged as the point where performance-based measures declined to zero or became net negative and where mortality rates increased sharply in acute stress assays. In this sense, T_c emerges as a unifying upper thermal limit that represent the physiological transition between sustained physiological function and damage that accumulates faster than it can be repaired.

For traits that are tightly linked to Darwinian fitness such as development, reproduction, and survival, the thermal performance in ectothermic organisms is positive only within the bounds of permissive temperatures, beyond which biological processes are disrupted (Huey & Kingsolver, 1989;

596 Angilletta, 2009; Fitter & Hay, 2012; Ørsted et al., 2022). Fitness-based performance metrics
597 therefore inherently reflects temperatures at which organisms can sustain homeostasis and complete
598 their life cycle. For both *L. gibba* and *D. suzukii*, we show that performance traits decline
599 progressively as temperatures approach the upper end of the permissive temperature range, but that
600 the point at which performance becomes net negative coincides with a sharp increase in the rate of
601 mortality measured in acute stress assays (Fig. 7). In *D. suzukii*, we observed that different
602 performance traits converged on similar T_c values, but exhibited subtle differences that likely reflect
603 variation in trait sensitivity across life stages (Rebolledo et al., 2020, 2021). Accordingly isolated
604 physiological traits may have different T_c, but when combined as a complete measure to characterise
605 completion of the lifecycle, it becomes the most sensitive trait that determines the apparent T_c. This
606 complexity suggests that T_c is not necessarily a fixed value, but rather a narrow temperature zone that
607 holds complexity that is specific to the life stage and activity of the organism. Accordingly, T_c may
608 not represent a single universal threshold applying equally across all traits within an organism (Ørsted
609 et al., 2022). Different traits, such as reproduction or growth, may differ in their sensitivity to thermal
610 stress (Angilletta, 2009; Kingsolver et al., 2011; Rebolledo et al., 2020, 2021; Ørsted et al., 2024;
611 Arnold et al., 2025) and thus might each have slightly different T_c values. Future studies that explicitly
612 estimate trait specific T_c values may therefore provide a more nuanced picture of thermal vulnerability
613 and help identify which functions most strongly limit performance and survival. Despite this trait-
614 level variation, the T_c estimates cluster within a narrow temperature zone and align with T_c inferred
615 from acute stress assays, supporting the interpretation that these measures unify at this same
616 underlying physiological transition. In *D. suzukii*, this transition reflects the sequential failure of
617 linked developmental and reproductive processes (egg development, larval growth, pupation, and
618 metamorphosis) that converge on upper thermal limits around ~29-31 °C (Fig. 7). These integrative
619 life history traits are more thermally sensitive than acute survival, consistent with evidence that

sterility and developmental failure occur below thermal limits (David et al., 2005; Walsh et al., 2019; Parratt et al., 2021; Ørsted et al., 2024). From a population perspective, these sublethal fitness limits may therefore be more relevant for population persistence than individual survival alone, even though fluctuating temperatures may buffer short-term exposure beyond these limits.

T_c can be approximated from shifts in thermal sensitivity and from the interaction between injury accumulation and recovery.

Although T_c has rarely been studied explicitly as a general physiological threshold, some experimental approaches have historically been used to relate shifts in thermal sensitivity to the interaction between injury accumulation and recovery. Early work on thermal limits in fish introduced chronic lethal or long-term survival thresholds that reflects the highest temperatures permitting sustained survival rather than acute failure (Fry et al., 1946; Fry, 1947; Fry, 1971). Similar transitions have been derived more recently through long-term survival limits in marine ectotherms (Richard et al., 2012). In parallel, modelling studies across both aquatic and terrestrial ectotherms further support the need for such a transition temperature, showing that time spent below a critical threshold during gradual warming does not contribute to injury accumulation (Kilgour et al., 1985; Kilgour & McCauley, 1986; Kingsolver & Umbanhowar, 2018; Jørgensen et al., 2021). Collectively, these studies motivate experimental approaches that resolve how survival time and mortality rates change across temperature, providing a practical basis for identifying T_c from shifts in thermal sensitivity.

Constant temperature assays can be used to characterise how survival time scales with temperature and to identify transitions between distinct physiological states. Traditionally, this approach has been used to examine temperature-dependent mortality using Arrhenius-type or semi-log plots of lifespan versus temperature, where changes in slope are interpreted as shifts in the processes governing

644 survival (Bigelow, 1921; Fry et al., 1946; Smith, 1957; Hollingsworth, 1969; Levitt, 1980; Cossins
645 & Bowler, 1987). Although such assays are often conducted at one or few temperatures, measuring
646 tolerance time across many temperatures allows assessing changes in thermal sensitivity, analogous
647 to Arrhenius analyses. Building on this framework, recent work within the TDT framework has
648 shown that the rate of mortality shifts from thermal sensitivities typical of biological rates at
649 permissive temperatures ($Q_{10} \sim 2$) to extremely high values at stressful temperatures ($Q_{10} \sim$ 100-
650 100.000), reflecting a transition from life-rate-limited to injury driven mortality (Smith, 1957;
651 Hollingsworth, 1969; Cossins & Bowler, 1987; Rezende et al., 2014; Jørgensen et al., 2019, 2022;
652 Ørsted et al., 2022; Holmstrup et al., 2023; Faber et al., 2024). In a comparative analysis, Jørgensen
653 et al. (2022) showed that plotting log death rate against temperature reveals a breakpoint
654 corresponding to T_c. Consistent with this framework, the constant temperature assays in the present
655 study revealed a pronounced breakpoint in the relationship between temperature and lifespan in both
656 study species (Fig. 4). Below T_c, mortality rates exhibited temperature dependence consistent with
657 normal biological processes ($Q_{10} \sim 2$; Gillooly et al., 2001; Brown et al., 2004; Dell et al., 2011;
658 Seebacher et al., 2015; Michaletz, 2018). Above T_c, mortality increased rapidly with increasing
659 temperature, consistent with the high thermal sensitivity associated with damage accumulation and
660 acute failure ($Q_{10} = 25044$ for *L. gibba* and $Q_{10} = 6754.97$ for *D. suzukii*). This breakpoint coincided
661 with the temperature range where developmental and reproductive performance became net positive
662 (Fig. 2, 3), demonstrating close agreement between T_c estimates from constant temperature and
663 performance-assays.
664
665 It is important to consider that prolonged exposure to constant temperatures does not reflect the
666 fluctuating thermal environments in nature. Ectotherms and plants are physiologically and
667 behaviourally adapted to variable temperatures (Kotak et al., 2007; Abram et al., 2017; Mody et al.,

2020; Guihur et al., 2022; Kefford et al., 2022; Jang et al., 2024), and heat stress responses can differ between day and night or between light and dark conditions (Havaux et al., 1991; Marutani et al., 2012; Tikkanen et al., 2018; Speights et al., 2017; Dadarwal et al., 2025). As a result, constant temperature assays can induce physiological states that may exaggerate or misrepresent T_c relative to natural conditions. Alternating constant temperature assays were recently proposed as a method of exploiting shifts in thermal sensitivity by combining brief exposures to stressful temperatures interrupted with recovery periods at lower temperatures to estimate T_c on short timescales (Fry et al., 1946; Cossins & Bowler, 1987; Ørsted et al., 2022, Ørsted et al., 2025). This approach assumes that thermal injury accumulates additively when the same damaging processes dominate across temperature intervals, whereas antagonistic effects may arise when different processes dominate in distinct thermal ranges (Fry et al., 1946; Colinet et al., 2015; Kovacevic et al., 2019; Jørgensen et al., 2022; Ørsted et al., 2022; Ørsted et al., 2025). Under these assumptions, extended survival during recovery phases can be used to identify permissive temperatures where damage accumulation is suppressed or partially reversed. Using this approach, the estimated T_c broadly matched those obtained from constant temperature and performance-based assays in both species (Fig. 7), supporting the interpretation that this method captures the same underlying physiological transition. However, the two species differed markedly in their recovery dynamics. In *L. gibba*, recovery periods did not measurably extend survival, and T_c was therefore identified primarily by a sharp increase in mortality rate at higher temperatures. In contrast, *D. suzukii* consistently survived longer when recovery periods occurred below T_c (Fig 6. B), suggesting rapid recovery and/or induction of transient heat hardening responses. Such short-term hardening effects are well documented in ectotherms and are often mediated by rapid induction stress-responses pathways, including heat shock proteins (Dahlgaard et al., 1998; Hoffman et al., 2010; Sgrò et al., 2010; Sørensen et al., 2019). Consequently, T_c estimates from alternating assays in *D. suzikii* were slightly elevated relative to other methods (Fig. 7), likely

692 because transient compensatory responses delayed failure at temperatures near the true physiological
693 transition. Collectively, alternating constant assays are practical (can be conducted within a single
694 day) and provide a biologically meaningful estimate of T_c that is comparable to constant temperature
695 and performance-based assays. More generally, moderately stressful recovery temperatures may
696 appear non-stressful during short exposures, but over longer durations they can contribute to
697 cumulative damage. As a result, T_c estimates from alternating assays tend to decrease when the
698 recovery period is extended, reflecting injury that was underestimated during too brief exposures.
699
700 **Ramping assays are not ideal for identifying T_c**
701 Ramping temperature assays involve gradually linear increasing temperatures until organisms
702 succumb to the stress at a final temperature (i.e., CT_{max}). In principle, varying the starting temperature
703 of these assays could allow T_c to be estimated as the temperature at which CT_{max} values begin to
704 increase across treatments. However, in practice, this approach does not work for either of the
705 organisms studied here. As the temperature increases linearly during ramping assays, thermal stress
706 accumulates exponentially with an extreme thermal sensitivity. Consequently, the majority of thermal
707 damage accumulation occurs at the most extreme temperatures reached during the ramps (well above
708 T_c), rather than being distributed evenly across the range of stressful temperatures above T_c. As an
709 example for *L. gibba*, during a linear ramp starting at 20 °C and increasing at 0.1 °C/min, only a tiny
710 fraction of total damage (~0.8% is accumulated by the time the ramp reaches T_c (38 °C), and roughly
711 10% of damage accumulates between 38 °C and ~42.8 °C. The vast majority of damage (~90%)
712 occurs at much higher temperatures (~42.8-45.1 °C), well above T_c, illustrating that damage is
713 concentrated at a few extreme temperatures. As a result, organisms experience little to no cumulative
714 damage at moderately stressful temperatures because exposure at those temperatures are too brief.
715 Temperatures that would otherwise induce significant stress or mortality after hours of exposure

716 therefore provide negligible contribution to accumulated damage during a ramp. This explains why
717 initiating ramps, even at temperatures well above T_c had no measurable effect on CT_{max} estimates in
718 both species. Overall, we therefore conclude that this assay is inappropriate for estimating T_c. That
719 being said, it should be possible to estimate T_c by using ramping assays with extremely slow ramping
720 rates since CT_{max} estimates should converge asymptotically towards T_c, as exposure time in the
721 stressful range increases for assays with slower ramp rates (Richard et al., 2012). Alternatively,
722 ramping with a non-linear rate, e.g. a progressively slower rate, would alleviate this issue by
723 distributing the injury accumulation per time unit evenly across the experiment, however to our
724 knowledge, no one has studied this in practice.
725

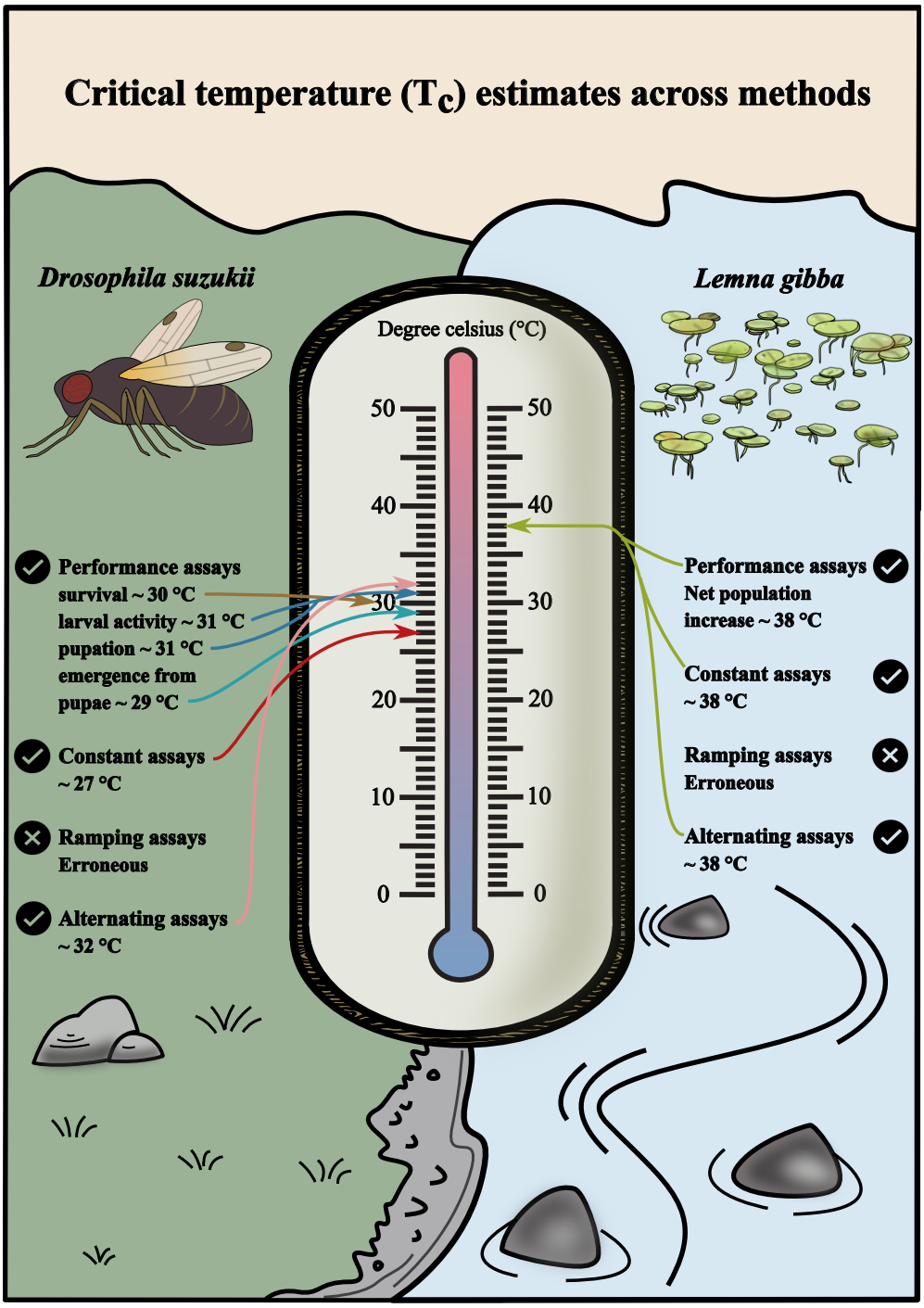

726

727

728 **Figure 7.** Critical temperature (T_c) estimates across methods for *Drosophila suzukii* (left) and *Lemna gibba* (right) across
729 four experimental methods. T_c represents the temperature at which the balance between homeostatic maintenance and
730 damage accumulation is equal, marking the transition from permissive to stressful conditions. In thermal performance
731 assays (conducted over several days), T_c was estimated for individual life-history traits in *D. suzukii* (egg laying, larval
732 activity, pupal development, and adult emergence from pupae) where each value indicates the upper temperature at which

that trait can successfully occur. For *L. gibba*, T_c was estimated from net population growth. Constant temperature assays (conducted over several days) estimated T_c from breakpoints in TDT models based on acute physiological failure (coma for flies, photosynthetic failure for duckweed), identifying the temperature above which mortality accelerates sharply. Ramping temperature assays (conducted within a single day) did not yield reliable T_c values because thermal damage accumulated predominantly at extreme temperatures rather than near the transition. Alternating constant temperature assays (conducted within a single day) combined brief exposures to stressful temperatures with recovery periods at lower, permissive temperatures. T_c was estimated as the temperature above which these recovery periods no longer slowed or reversed damage accumulation, resulting in rapid onset of failure (coma for flies, photosynthetic failure for duckweed), capturing the upper thermal limit at which compensatory or repair mechanisms can no longer maintain homeostasis. These estimates collectively illustrate how T_c varies across traits, methods, and species, highlighting differences in thermal sensitivity and recovery dynamics.

Conflict of interest

This work has no conflict of interests.

Literature

Abram, P. K., Boivin, G., Moiroux, J., & Brodeur, J. (2017). Behavioural effects of temperature on ectothermic animals: unifying thermal physiology and behavioural plasticity. Biological Reviews, 92(4), 1859-1876.

Alexandrov, V. Y. (1964). Cytophysiological and cytoecological investigations of heat resistance of plant cells toward the action of high and low temperature. Quarterly Review of Biology 39, 35–77.

Arnold, P. A., Noble, D. W., Nicotra, A. B., Kearney, M. R., Rezende, E. L., Andrew, S. C., ... & Bennett, J. M. (2025). A framework for modelling thermal load sensitivity across life. Global Change Biology, 31(7), e70315.

Angilletta Jr, M. J. (2009). Thermal adaptation: a theoretical and empirical synthesis. Oxford Univ. Press.

Bennett, J. M., Sunday, J., Calosi, P., Villalobos, F., Martínez, B., Molina-Venegas, R., ... & Olalla-Tárraga, M. Á. (2021). The evolution of critical thermal limits of life on Earth. Nature communications, 12(1), 1198.

Berry, J., & Bjorkman, O. (1980). Photosynthetic response and adaptation to temperature in higher plants. Annu Rev Plant Physiol. 31: 491–543.

Bigelow, W. (1921). The logarithmic nature of thermal death time curves. The Journal of Infectious Diseases, 528-536.

Briceño, V. F., Arnold, P. A., Cook, A. M., Courtney Jones, S. K., Gallagher, R. V., French, K., ... & Leigh, A. (2025). Drivers of thermal tolerance breadth of plants across contrasting biomes. Journal of Ecology.

Brown, J. H., Gillooly, J. F., Allen, A. P., Savage, V. M., & West, G. B. (2004). Toward a metabolic theory of ecology. Ecology, 85(7), 1771-1789.

Buckley, L. B., Huey, R. B., & Kingsolver, J. G. (2022). Asymmetry of thermal sensitivity and the thermal risk of climate change. Global Ecology and Biogeography, 31(11), 2231-2244.

Colinet, H., Sinclair, B. J., Vernon, P., & Renault, D. (2015). Insects in fluctuating thermal environments. Annual review of entomology, 60, 123-140.

Collander, R. (1924). Beobachtungen uber die quantitativen Beziehungen zwischen Totungsgeschwindigkeit und Temperatur beim Warmetod pflan- zlicher Zellen. Commentationes Biologicae Societas Scientiarum Fennica 1, 1–12.

Cook, A. M., Rezende, E. L., Petrou, K., & Leigh, A. (2024). Beyond a single temperature threshold: Applying a cumulative thermal stress framework to plant heat tolerance. Ecology Letters, 27(3), e14416.

Cossins A. R., Bowler K. (1987). Temperature biology of animals. London: Chapman and Hall.

807 Dadarwal, B. K., Yadav, N., Chauhan, J., & Singhal, R. K. (2025). Plant Growth and Development
808 Under High Night Temperatures. In Impact of High Night Temperature on Plant Biology (pp. 31-50).
809 Apple Academic Press.
810
811 Dahlgaard, J., Loeschcke, V., Michalak, P., & Justesen, J. (1998). Induced thermotolerance and
812 associated expression of the heat-shock protein Hsp70 in adult Drosophila melanogaster. Functional
813 Ecology, 12(5), 786-793.
814
815 David, J. R., Araripe, L. O., Chakir, M., Legout, H., Lemos, B., Pétavy, G., ... & Moreteau, B. (2005).
816 Male sterility at extreme temperatures: a significant but neglected phenomenon for understanding
817 Drosophila climatic adaptations. Journal of evolutionary biology, 18(4), 838-846.
818
819 Dell, A. I., Pawar, S., & Savage, V. M. (2011). Systematic variation in the temperature dependence
820 of physiological and ecological traits. Proceedings of the National Academy of Sciences, 108(26),
821 10591-10596.
822
823 Deutsch, C. A., Tewksbury, J. J., Huey, R. B., Sheldon, K. S., Ghalambor, C. K., Haak, D. C., &
824 Martin, P. R. (2008). Impacts of climate warming on terrestrial ectotherms across latitude.
825 Proceedings of the National Academy of Sciences, 105(18), 6668-6672.
826
827 Diamond, S. E. (2017). Evolutionary potential of upper thermal tolerance: biogeographic patterns and
828 expectations under climate change. Annals of the New York Academy of Sciences, 1389(1), 5-19.
829

Downton, W. J. S., Berry J. A., (1982). Chlorophyll fluorescence at high temperature. Biochim Biophys Acta. 679: 474–478.

Faber, A. H., Ørsted, M., & Ehlers, B. K. (2024). Application of the thermal death time model in predicting thermal damage accumulation in plants. Journal of Experimental Botany, 75(11), 3467-3482.

Fitter, A. H., & Hay, R. K. (2012). Environmental physiology of plants. Academic press.

Fry, F. E. J. (1947). Effects of the environment on animal activity. Publications of the Ontario Fisheries Research Laboratory 55, 1-62

Fry, F. E. J. (1971). The effect of environmental factors on the physiology of fish. Fish Physiol. 6, 1-98. doi:10.1016/S1546-5098(08)60146-6

Fry, F. E. J., Hart, J. S., & Walker, K. F. (1946). Lethal temperature relations for a sample of young speckled trout. University of Toronto Studies, Biological Series, 54, 9-35.

Gillooly, J. F., Brown, J. H., West, G. B., Savage, V. M., & Charnov, E. L. (2001). Effects of size and temperature on metabolic rate. science, 293(5538), 2248-2251.

Guihur, A., Rebeaud, M. E., & Goloubinoff, P. (2022). How do plants feel the heat and survive?. Trends in biochemical sciences, 47(10), 824-838.

Havaux, M., Greppin, H., & Strasser, R. J. (1991). Functioning of photosystems I and II in pea leaves exposed to heat stress in the presence or absence of light: Analysis using in-vivo fluorescence, absorbance, oxygen and photoacoustic measurements. Planta, 186, 88-98.

Huey, R. B., & Kingsolver, J. G. (1989). Evolution of thermal sensitivity of ectotherm performance. Trends in ecology & evolution, 4(5), 131-135.

Hoffmann, G. E., & Todgham, A. E. (2010). Living in the now: physiological mechanisms to tolerate a rapidly changing environment. Annual review of physiology, 72(1), 127-145.

Hollingsworth, M. J. (1969). Temperature and length of life in Drosophila. Experimental Gerontology, 4(1), 49-55.

Holmstrup, M., Touzot, M., & Slotsbo, S. (2023). Characterization of the thermal death time landscape for Enchytraeus albidus. Pedobiologia, 97, 150876.

IPCC. (2023) In: Core Writing Team, H. Lee & J. Romero (Eds) Climate change 2023: synthesis report. Contribution of Working Groups I, II and III to the sixth assessment report of the Intergovernmental Panel on Climate Change. Geneva, Switzerland: IPCC, PP. 35-115.

Jang, J., Lee, S., Kim, J. I., Lee, S., & Kim, J. A. (2024). The roles of circadian clock genes in plant temperature stress responses. International Journal of Molecular Sciences, 25(2), 918.

877 Jørgensen, L. B., Malte, H., & Overgaard, J. (2019). How to assess Drosophila heat tolerance:
878 Unifying static and dynamic tolerance assays to predict heat distribution limits. Functional Ecology,
879 33(4), 629-642.
880
881 Jørgensen, L. B., Malte, H., Ørsted, M., Klahn, N. A., & Overgaard, J. (2021). A unifying model to
882 estimate thermal tolerance limits in ectotherms across static, dynamic and fluctuating exposures to
883 thermal stress. Scientific Reports, 11(1), 12840.
884
885 Jørgensen, L. B., Robertson, R. M., & Overgaard, J. (2020). Neural dysfunction correlates with heat
886 coma and CTmax in Drosophila but does not set the boundaries for heat stress survival. Journal of
887 Experimental Biology, 223(13), jeb218750.
888
889 Jørgensen, L. B., Ørsted, M., Malte, H., Wang, T., & Overgaard, J. (2022). Extreme escalation of
890 heat failure rates in ectotherms with global warming. Nature, 611(7934), 93-98.
891
892 Kearney, M., & Porter, W. (2009). Mechanistic niche modelling: combining physiological and spatial
893 data to predict species' ranges. Ecology letters, 12(4), 334-350.
894
895 Kefford, B. J., Ghalambor, C. K., Dewenter, B., Poff, N. L., Hughes, J., Reich, J., & Thompson, R.
896 (2022). Acute, diel, and annual temperature variability and the thermal biology of ectotherms. Global
897 Change Biology, 28(23), 6872-6888.
898
899 Kellermann, V., Overgaard, J., Hoffmann, A. A., Fløjgaard, C., Svenning, J. C., & Loeschcke, V.
900 (2012). Upper thermal limits of Drosophila are linked to species distributions and strongly

901 constrained phylogenetically. Proceedings of the National Academy of Sciences, 109(40), 16228-
902 16233.
903
904 Knight, C. A., & Ackerly, D. D. (2003). Evolution and plasticity of photosynthetic thermal tolerance,
905 specific leaf area and leaf size: congeneric species from desert and coastal environments. New Phytol.
906 160: 337–347.
907
908 Kilgour, D. M., & McCauley, R. W. (1986). Reconciling the two methods of measuring upper lethal
909 temperatures in fishes. Environmental Biology of Fishes, 17(4), 281-290.
910
911 Kilgour, D. M., McCauley, R. W., & Kwain, W. (1985). Modeling the lethal effects of high
912 temperature on fish. Canadian Journal of Fisheries and Aquatic Sciences, 42(5), 947-951.
913
914 Kingsolver, J. G., Arthur Woods, H., Buckley, L. B., Potter, K. A., MacLean, H. J., & Higgins, J. K.
915 (2011). Complex life cycles and the responses of insects to climate change.
916
917 Kingsolver, J. G., & Umbanhowar, J. (2018). The analysis and interpretation of critical temperatures.
918 Journal of Experimental Biology, 221(12), jeb167858.
919
920 Kotak, S., Larkindale, J., Lee, U., von Koskull-Döring, P., Vierling, E., & Scharf, K. D. (2007).
921 Complexity of the heat stress response in plants. Current opinion in plant biology, 10(3), 310-316.
922
923 Kovacevic, A., Latombe, G., & Chown, S. L. (2019). Rate dynamics of ectotherm responses to
924 thermal stress. Proceedings of the royal society B, 286(1902), 20190174.

925

926 Lancaster, L. T., & Humphreys, A. M. (2020). Global variation in the thermal tolerances of plants.
927 Proceedings of the National Academy of Sciences, 117(24), 13580-13587.

928

929 Levitt J. (1980). Responses of plants to environmental stress, Volume 1: Chilling, freezing, and high
930 temperature stresses. New York: Academic Press.

931

932 Malusare, S. P., Zilio, G., & Fronhofer, E. A. (2023). Evolution of thermal performance curves: A
933 meta-analysis of selection experiments. Journal of Evolutionary Biology, 36(1), 15-28.

934

935 Marutani, Y., Yamauchi, Y., Kimura, Y., Mizutani, M., & Sugimoto, Y. (2012). Damage to
936 photosystem II due to heat stress without light-driven electron flow: involvement of enhanced
937 introduction of reducing power into thylakoid membranes. Planta, 236, 753-761.

938

939 Michaletz, S. T. (2018). Evaluating the kinetic basis of plant growth from organs to ecosystems. New
940 phytologist, 219(1), 37-44.

941

942 Mody, T., Bonnot, T., & Nagel, D. H. (2020). Interaction between the circadian clock and regulators
943 of heat stress responses in plants. Genes, 11(2), 156.

944

945 Muggeo, V. M. (2008). Segmented: an R package to fit regression models with broken-line
946 relationships. R news, 8(1), 20-25.

947

948 Neuner, G., & Buchner, O. (2023). The dose makes the poison: the longer the heat lasts, the lower
949 the temperature for functional impairment and damage. Environmental and Experimental Botany,
950 212, 105395.
951
952 Parratt, S. R., Walsh, B. S., Metelmann, S., White, N., Manser, A., Bretman, A. J., ... & Price, T. A.
953 (2021). Temperatures that sterilize males better match global species distributions than lethal
954 temperatures. Nature Climate Change, 11(6), 481-484.
955
956 Pörtner, H. O., & Farrell, A. P. (2008). Physiology and climate change. Science, 322(5902), 690-692.
957
958 Rebolledo, A. P., Sgrò, C. M., & Monro, K. (2020). Thermal performance curves reveal shifts in
959 optima, limits and breadth in early life. Journal of Experimental Biology, 223(22), jeb233254.
960
961 Rebolledo, A. P., Sgrò, C. M., & Monro, K. (2021). Thermal performance curves are shaped by prior
962 thermal environment in early life. Frontiers in Physiology, 12, 738338.
963
964 Rezende, E. L., Castañeda, L. E., & Santos, M. (2014). Tolerance landscapes in thermal ecology.
965 Functional Ecology, 28(4), 799-809.
966
967 Richard, J., Morley, S. A., Thorne, M. A., & Peck, L. S. (2012). Estimating long-term survival
968 temperatures at the assemblage level in the marine environment: towards macrophysiology. PLoS
969 One, 7(4), e34655.
970

971 Sastry A., & Barua, D. (2017). Leaf thermotolerance in tropical trees from a seasonally dry climate
972 varies along the slow–fast resource acquisition spectrum. Scientific Reports. 7: 11246.
973
974 Schoolfield, R. M., Sharpe, P. J. H., & Magnuson, C. E. (1981). Non-linear regression of biological
975 temperature-dependent rate models based on absolute reaction-rate theory. Journal of theoretical
976 biology, 88(4), 719-731.
977
978 Schreiber U, Berry JA. 1977. Heat-induced changes of chlorophyll fluorescence in intact leaves
979 correlated with damage of the photosynthetic apparatus. Planta. 136: 233–238.
980
981 Schulte, P. M. (2015). The effects of temperature on aerobic metabolism: towards a mechanistic
982 understanding of the responses of ectotherms to a changing environment. The Journal of experimental
983 biology, 218(12), 1856-1866.
984
985 Schulte, P. M., Healy, T. M., & Fangue, N. A. (2011). Thermal performance curves, phenotypic
986 plasticity, and the time scales of temperature exposure. Integrative and comparative biology, 51(5),
987 691-702.
988
989 Seebacher, F., White, C. R., & Franklin, C. E. (2015). Physiological plasticity increases resilience of
990 ectothermic animals to climate change. Nature Climate Change, 5(1), 61-66.
991
992 Sgrò, C. M., Overgaard, J., Kristensen, T. N., Mitchell, K. A., Cockerell, F. E., & Hoffmann, A. A.
993 (2010). A comprehensive assessment of geographic variation in heat tolerance and hardening capacity

994 in populations of Drosophila melanogaster from eastern Australia. Journal of evolutionary biology,
995 23(11), 2484-2493.
996
997 Smith, J. M. (1957). Temperature tolerance and acclimatization in Drosophila subobscura. Journal of
998 Experimental Biology, 34(1), 85-96.
999
1000 Speights, C. J., Harmon, J. P., & Barton, B. T. (2017). Contrasting the potential effects of daytime
1001 versus nighttime warming on insects. Current Opinion in Insect Science, 23, 1-6.
1002
1003 Sunday, J. M., Bates, A. E., & Dulvy, N. K. (2011). Global analysis of thermal tolerance and latitude
1004 in ectotherms. Proceedings of the Royal Society B: Biological Sciences, 278(1713), 1823-1830.
1005
1006 Sørensen, M. H., Kristensen, T. N., Lauritzen, J. M. S., Noer, N. K., Høye, T. T., & Bahrndorff, S.
1007 (2019). Rapid induction of the heat hardening response in an Arctic insect. Biology Letters, 15(10),
1008 20190613.
1009
1010 Tikkanen, M., & Grebe, S. (2018). Switching off photoprotection of photosystem I–a novel tool for
1011 gradual PSI photoinhibition. Physiologia Plantarum, 162(2), 156-161.
1012
1013 Walsh, B. S., Parratt, S. R., Hoffmann, A. A., Atkinson, D., Snook, R. R., Bretman, A., & Price, T.
1014 A. (2019). The impact of climate change on fertility. Trends in Ecology & Evolution, 34(3), 249-259.
1015 Wood, S. N. 2017. Generalized additive models: an introduction with R. Boca Raton, FL, USA: CRC
1016 Press.

1017 Ørsted, M., Jørgensen, L., Hůla, P., & Overgaard, J. (2025). Integrating physiological rates of thermal
1018 stress and repair predicts heat failure during temperature fluctuations. Authorea Preprints.
1019
1020 Ørsted, M., Jørgensen, L. B., & Overgaard, J. (2022). Finding the right thermal limit: a framework to
1021 reconcile ecological, physiological and methodological aspects of CTmax in ectotherms. Journal of
1022 Experimental Biology, 225(19), jeb244514.
1023
1024 Ørsted, M., Willot, Q., Olsen, A. K., Kongsgaard, V., & Overgaard, J. (2024). Thermal limits of
1025 survival and reproduction depend on stress duration: A case study of Drosophila suzukii. Ecology
1026 Letters, 27(3), e14421

Supporting information

Article title: Separating good from bad – a methodological assessment of the critical temperature that separates stressful and permissive temperatures in ectotherms.

The following Supporting Information is available for this article:

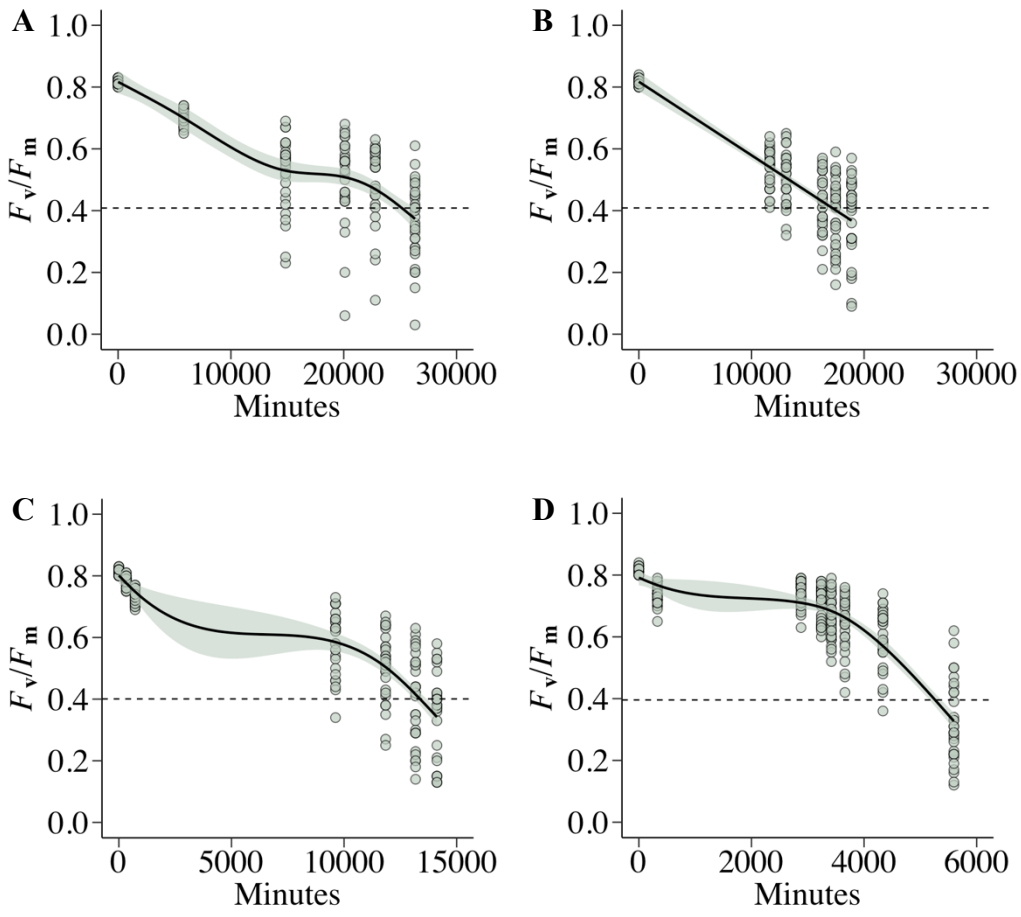

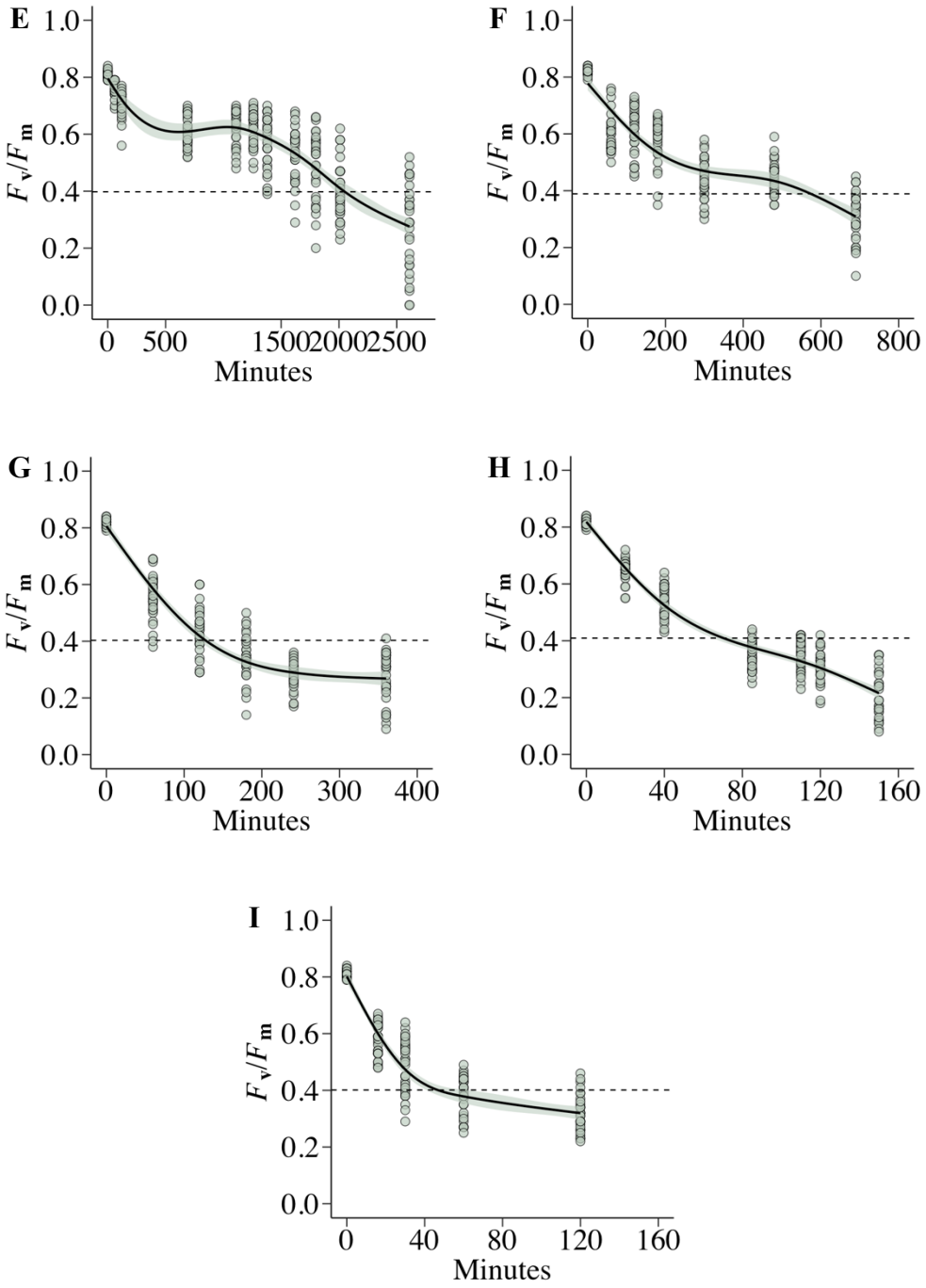

Figure S1. Estimation of thermal failure times for all constant temperature for *Lemna gibba*. Generalized additive models (GAMs) were fitted to the maximum quantum efficiency (F_v/F_m) of PSII as a function of stress duration for each assay. The fitted GAMs (black lines) show the estimated decline in F_v/F_m, and vertical dashed lines indicate the time point at which F_v/F_m dropped by 50%, defining the time of thermal failure. The assays are labelled according to their temperature: **A**) 36, **B**) 37, **C**) 38, **D**) 39 and **E**) 40, **F**) 41, **G**) 42, **H**) 43 and **I**) 44 °C, and the thermal failure estimates are identical to those shown in **Fig. 2A**.

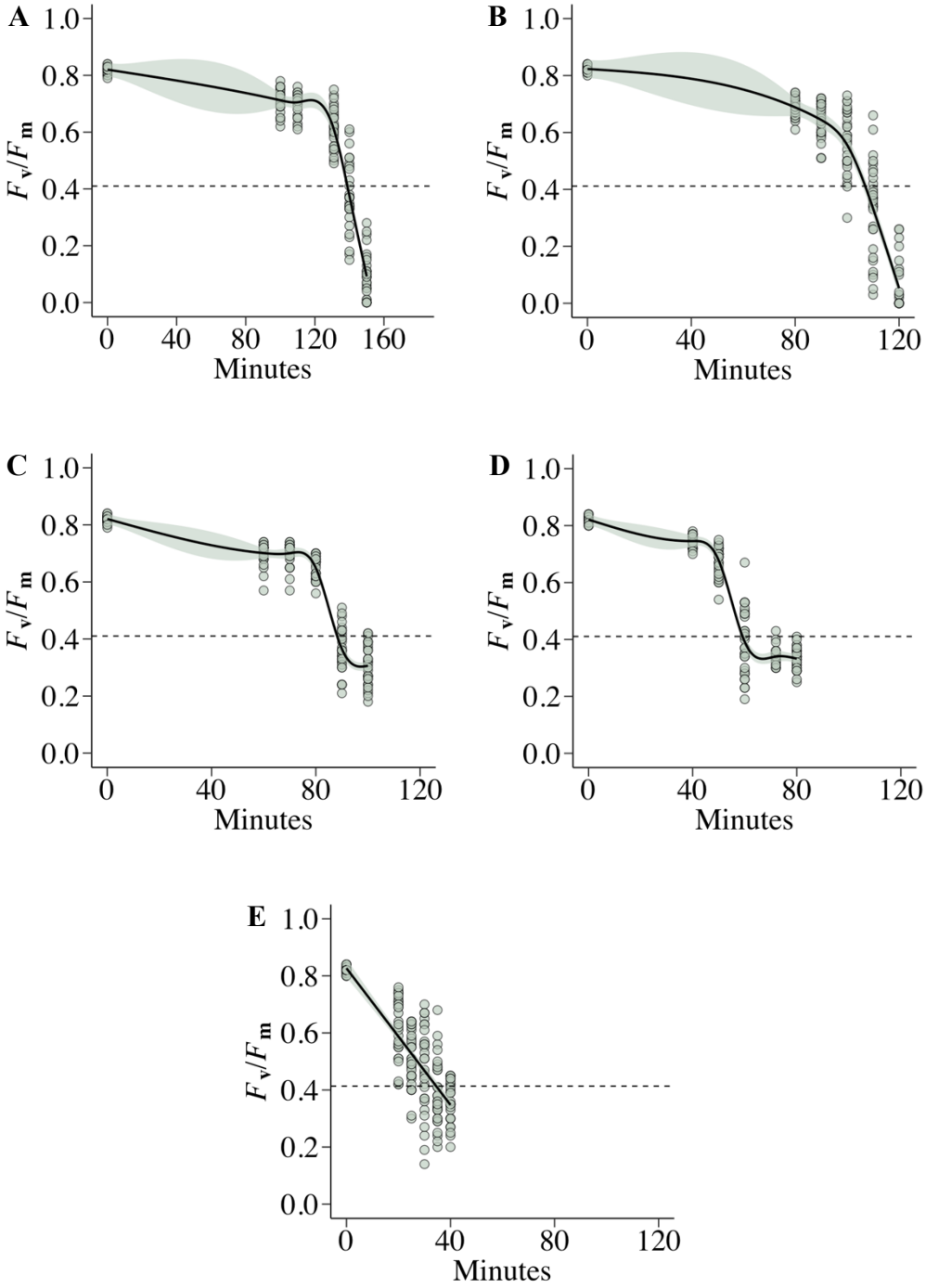

Figure S2. Estimation of thermal failure times for all ramping assays with different starting temperatures for *Lemna gibba*. Generalized additive models (GAMs) were fitted to the maximum quantum efficiency (F_v/F_m) of PSII as a function of stress duration for each assay. The fitted GAMs (black lines) show the estimated decline in F_v/F_m, and vertical dashed lines indicate the time point at which F_v/F_m dropped by 50%, defining the time of thermal failure. Assays were initiated at different starting temperatures and then the temperature was increased in a linear fashion (0.15 °C/min). The assays are labelled according to their stating temperature: **A**) 26, **B**) 30, **C**) 34, **D**) 38 and **E**) 42 °C, and the thermal failure estimates are identical to those shown in **Fig. 3A**.

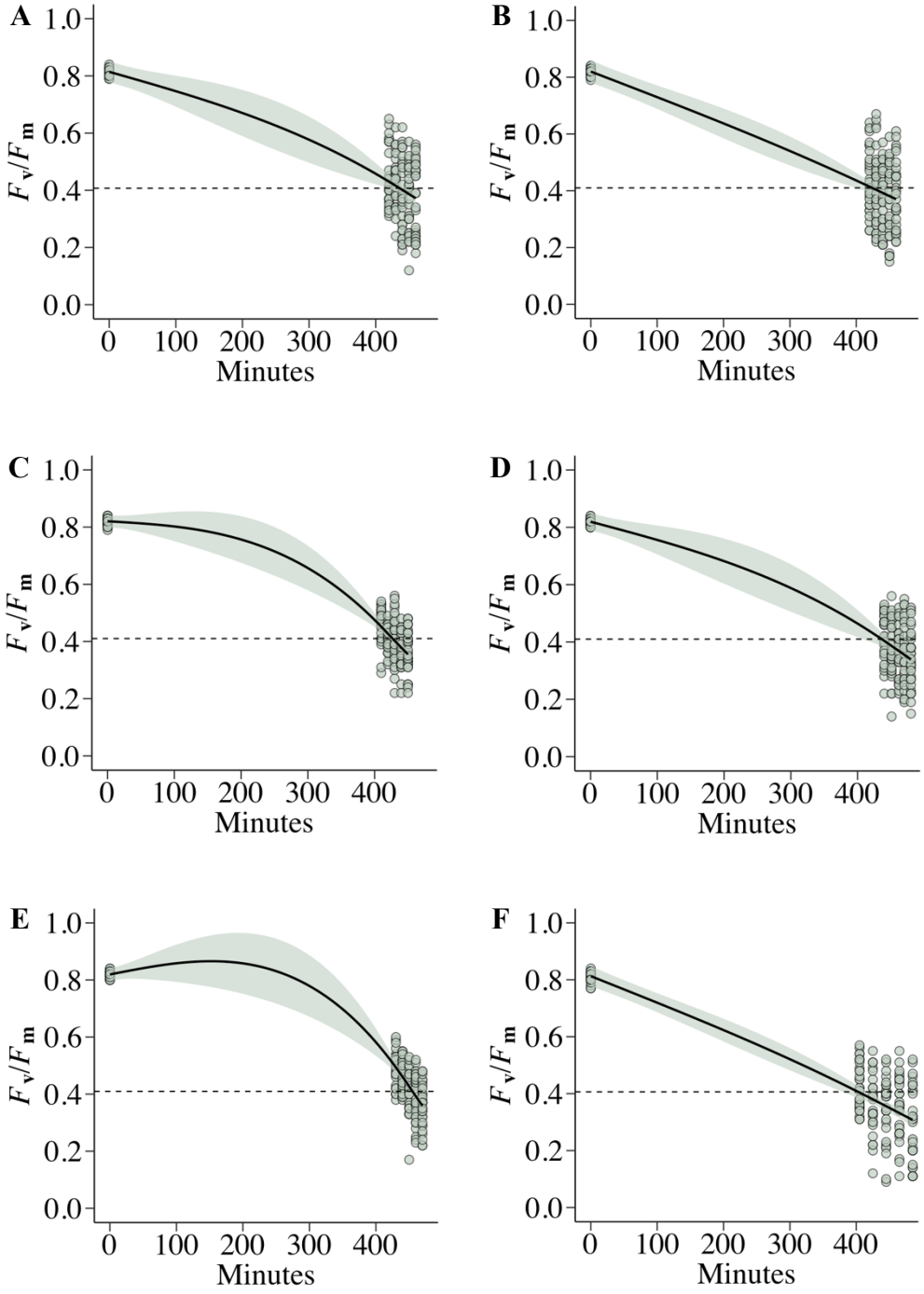
A
B
C
D
E
F
F_v/F_m
1.0
0.8
0.6
0.4
0.2
0.0
0
100
200
300
400
Minutes

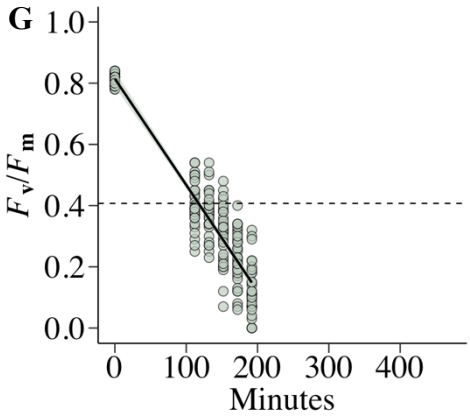

Figure S3. Estimation of thermal failure times for all alternating constant temperature assays with different starting temperatures for *Lemna gibba*. Generalized additive models (GAMs) were fitted to the maximum quantum efficiency (F_v/F_m) of PSII as a function of stress duration for each assay. The fitted GAMs (black lines) show the estimated decline in F_v/F_m, and vertical dashed lines indicate the time point at which F_v/F_m dropped by 50%, defining the time of thermal failure. Individuals were initially exposed to a stressful high temperature (43 °C) for a duration resulting in approximately 50 percent damage determined by the thermal death time (TDT) models in **Fig. 2A**. This was followed by a temperature drop to a single lower temperature between 26 and 42 °C for six hours. After this period, individuals were returned to the initial stressful temperature until thermal failure occurred, if not already reached. The assays are labelled according to the temperature used for the temperature drops: **A**) 26, **B**) 30, **C**) 34, **D**) 36, **E**) 38, **F**) 40 and **G**) 42 °C and the thermal failure estimates are identical to those shown in **Fig. 4A**.